SynthForensics: A Multi-Generator Benchmark for Detecting Synthetic Video Deepfakes

Roberto Leotta*
iCTLab s.r.l.

Salvatore Alfio Sambataro*
University of Catania

Claudio Vittorio Ragaglia
University of Catania

Mirko Casu
University of Catania

Yuri Petralia
iCTLab s.r.l.

Francesco Guarnera
University of Catania

Luca Guarnera
University of Catania

Sebastiano Battiato
University of Catania

{roberto.leotta, yuri.petralia}@ictlab.srl
{salvatore.sambataro, claudio.ragaglia, mirko.casu}@phd.unict.it
{francesco.guarnera, luca.guarnera, sebastiano.battiato}@unict.it

*These authors contributed equally to this work.
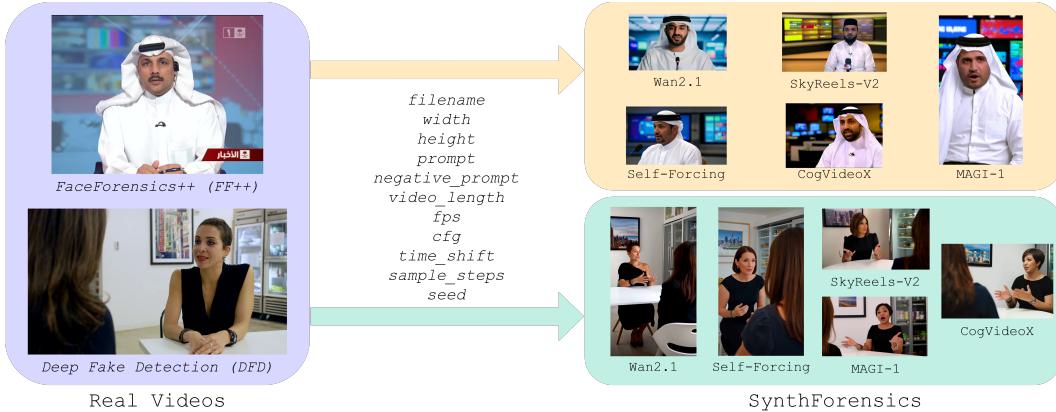
Figure 1. The paired-source data generation pipeline for SynthForensics. Real source videos (left) from FF++ and DFD are analyzed to extract structured metadata, which guides five text-to-video (T2V) models (Wan2.1, SkyReels-V2, Self-Forcing, CogVideoX, MAGI-1) to generate synthetic counterparts (right).

Abstract

The landscape of synthetic media has been irrevocably altered by text-to-video (T2V) models, whose outputs are rapidly approaching indistinguishability from reality. Critically, this technology is no longer confined to large-scale labs; the proliferation of efficient, open-source generators is democratizing the ability to create high-fidelity synthetic content on consumer-grade hardware. This makes existing face-centric and manipulation-based benchmarks obsolete. To address this urgent threat, we introduce SynthForensics, to the best of our knowledge the first human-centric benchmark for detecting purely synthetic video deepfakes. The benchmark comprises 6,815 unique videos from five architecturally distinct, state-of-the-art open-source T2V models. Its construction was underpinned by a meticulous two-stage, human-in-the-loop validation to ensure high semantic and visual quality. Each video is provided in four versions (raw, lossless, light, and heavy compression) to enable real-world robustness testing. Experiments demonstrate that state-of-the-art detectors are both fragile and exhibit limited generalization when evaluated on this new domain: we observe a mean performance drop of 29.19% AUC, with some methods performing worse than random chance, and top models losing over 30 points under heavy compression. The paper further investigates the efficacy of training on SynthForensics as a means to mitigate these observed performance gaps, achieving robust generalization to unseen generators (93.81% AUC), though at the cost of reduced backward compatibility with traditional

manipulation-based deepfakes. The complete dataset and all generation metadata, including the specific prompts and inference parameters for every video, will be made publicly available at [link anonymized for review].

1. Introduction

Text-to-video (T2V) models have transformed synthetic media creation, with outputs now approaching photorealism. While closed-source models like Sora 2 [40], VEO 3.1 [16], and Kling 2.5 [30] define the state-of-the-art, efficient open-source generators are democratizing high-fidelity synthesis on consumer-grade hardware [24]. This presents an urgent threat: video forensics must now confront content that is born synthetic, not merely altered.

Existing benchmarks (FaceForensics++ [45], Celeb-DF [32], DFDC [12]) were designed for manipulation detection, not pure synthesis. Their face-centric scope and specialization in alteration artifacts render them inadequate for modern T2V outputs. Public benchmarks for open-source T2V models are nearly absent, creating urgent need for human-centric resources capturing the full diversity of modern synthetic video [31]. To address this gap, we introduce SynthForensics, the first human-centric benchmark for purely synthetic video detection, comprising 6,815 unique videos from five architecturally diverse, state-of-the-art open-source T2V models, totaling over ~9.5 hours of content and 550,000+ frames. The benchmark incorporates several key innovations. First, it features significant generation diversity with varying resolutions, frame rates, durations, landscape and portrait aspect ratios to systematically incorporate modern video platform formats. Second, it employs a rigorous 1-to-1 paired-source generation protocol, where each synthetic video is generated from a structured prompt derived from a real source video (Figure 1). This design aims to control for high-level semantic variables, minimizing content-based confounds and encouraging detectors to learn generative artifacts rather than semantic correlations. Third, its construction was underpinned by extensive human-in-the-loop validation: every prompt was manually validated for semantic fidelity and ethics, and every video was inspected for quality, coherence, and ethical compliance. Finally, we provide each video in four versions (raw, lossless, light and heavy compression) alongside comprehensive metadata (prompts and generation parameters) for full reproducibility. Figure 2 shows our pipeline. Our main contributions are:

- We introduce SynthForensics, the first human-centric benchmark for purely synthetic video detection, built on paired-source protocol with five diverse T2V models and extensive human validation.
- We conduct comprehensive evaluation quantifying state-of-the-art detector failures and demonstrating dataset

learnability through training experiments, revealing strong forward generalization but severe backward incompatibility with manipulation-based deepfakes.
- We publicly release the complete benchmark across four variants with full generation details for reproducibility.

Section 2 reviews related work. Section 3 details methodology. Section 4 describes experimental protocols. Section 9 presents results on zero-shot performance, compression robustness, training efficacy, and generalization. Section 6 concludes with discussion, limitations, and future work.
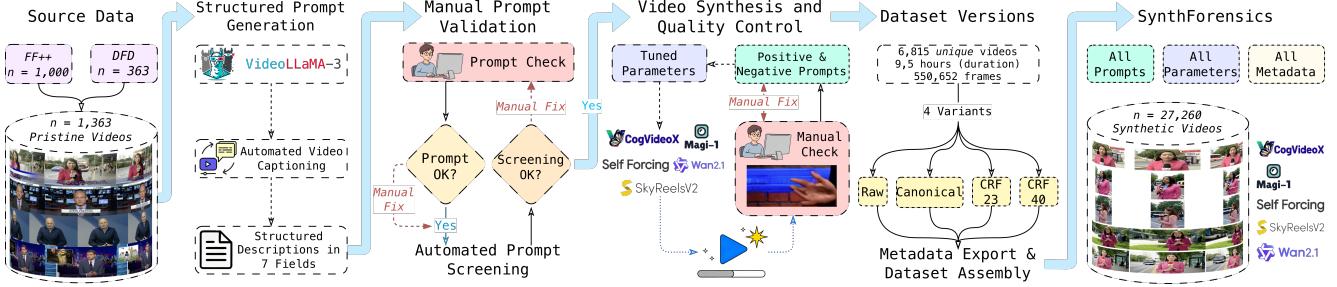
2. Related Work

The following section reviews the architectural evolution from early generative models to modern T2V systems, and surveys existing detection benchmarks and methodologies. This contextualization highlights the gap: current datasets focus on manipulation rather than pure synthesis.

2.1. The Evolution of Generative Video Models

The development of synthetic video has progressed through several key phases. GANs [15] enabled the first realistic face manipulations through adversarial training. Subsequently, Diffusion Models (DM) [22] improved visual fidelity through iterative denoising, quickly becoming the dominant paradigm for controllable image and video synthesis [18, 43, 46, 57], raising societal concerns such as the erosion of trust in multimedia [6].

Recent T2V systems converge on the Diffusion Transformer (DiT) paradigm [41], which replaces convolutional U-Nets [44] with transformer architectures [48] for spatio-temporal diffusion. This enables superior long-range coherence and scalability to billions of parameters. Within this landscape, open-source models have rapidly expanded T2V capabilities through architectural innovations and training optimizations. For instance, HunyuanVideo [28] introduced multi-dimensional structured prompting with MLLMs alongside a Transformer-based full-attention mechanism and causal 3D VAE. CausVid [55] introduced efficient autoregressive diffusion with causal dependencies. Additional efforts focused on efficiency and quality: LTX-Video [19] optimized for real-time latency, Step-Video-T2V [38] integrated Flow Matching [35] and Video-DPO [36] for human preference alignment, and OpenSora 2.0 [42] aimed to replicate proprietary model scale through systematic optimization and efficient resource allocation. Among these innovations, five models stand out for their architectural diversity and widespread adoption. Wan2.1 (14B parameters) [49] implements a specialized spatio-temporal VAE within a standard DiT architecture for high-resolution output and frame consistency. CogVideoX-5B (5B parameters) [54] employs an Expert Transformer with specialized adaptive normalization for separate text-vision processing alongside a 3D VAE with temporal com-

Figure 2. **The SynthForensics benchmark.** Starting from 1,363 source videos (FF++, DFD), a VLM generates structured 7-field descriptions validated by human reviewers. Each prompt is optimized for five T2V models (CogVideoX, MAGI-1, Self-Forcing, SkyReels-V2, Wan2.1). Synthesized videos undergo human validation before processing into four compression versions (Raw, Canonical, CRF23, CRF40). The final benchmark comprises 6,815 unique videos (27,260 total) with full metadata (prompts, parameters) for reproducibility.

pression. SkyReels-V2 (14B parameters) [7] integrates reinforcement learning and diffusion forcing within its DiT architecture for advanced temporal coherence. Self-Forcing (1.3B parameters) [23], using a causal DiT architecture, introduces self-rollout with key-value (KV) caching during training to solve exposure bias, enabling real-time streaming on consumer GPUs [24]. MAGI-1-Distilled (24B parameters) [1], referred to as MAGI-1, represents a pure autoregressive approach with chunk-based generation and strict causality.

2.2. Benchmarks for Video Deepfake Detection

The deepfake detection landscape has been shaped by manipulation-focused datasets, with several benchmarks introduced for this purpose. Rössler et al. [45] released *Face-Forensics++* (FF++), comprising YouTube videos manipulated via four methods for identity replacement and expression reenactment. The *Deep Fake Detection* (DFD) dataset [14] adds 363 pristine videos and ∼3,000 manipulations from 28 actors for cross-dataset evaluation. Li et al. [32] proposed *Celeb-DF* (CDF), improving synthesis quality through higher resolution, refined blending, and temporal smoothing, later expanded in *Celeb-DF++* [33]. Additional manipulation benchmarks include *TIMIT* [29] with GAN-based face swaps in dual quality levels, *DFDC* [12] with extensive post-processing for real-world approximation, *DeeperForensics-1.0* [26] with DF-VAE forgeries and perturbations, *WildDeepfake* [59] with in-the-wild samples, and *TM* [8] with audiovisual manipulations and Asian demographic focus. More recently, *AV-Deepfake1M++* [4] extends audio-visual manipulation with LLM-driven content editing using multiple TTS and lip-sync models alongside real-world perturbations. Recent benchmarks for synthetic video [2, 3, 39] focus on action semantics, general video re-generation, or non-human content, making them unsuitable for evaluating detectors on high-fidelity, human-centric T2V scenarios.

2.3. Deepfake Detection Methodologies

Deepfake detection research has evolved along two primary methodological lines: frame-level analysis, which treats video as a collection of independent images, and video-level analysis, which explicitly models temporal dynamics. Frame-level detectors aim to identify spatial artifacts within individual frames. This family includes approaches based on metric learning CFM [37], reconstruction learning RECCE [5], progressive learning ProDet [10], and feature disentanglement UCF [51]. Recent approaches employ Vision Transformer (ViT) [13] architectures like Effort [53]. Video-level detectors produce a single verdict for an entire video. Advanced methods integrate temporal analysis directly into their architecture. AltFreezing [50] alternates the training of spatial and temporal convolutional weights to capture both types of artifacts, while FTCN [58] employs fully temporal convolutions to focus exclusively on temporal inconsistencies. Recent approaches leverage Vision Transformer architectures GenConViT [11] or adapt foundation models DFD-FCG [20] to actively model spatio-temporal patterns.

3. The SynthForensics Benchmark

This section details the SynthForensics construction pipeline, visually summarized in Figure 2.

3.1. Source Data and Generative Models

SynthForensics employs a paired-source protocol using 1,363 pristine videos from FF++ [45] (1,000 videos) and DFD [14] (363 videos). Each pristine video serves as anchor for generating a corresponding synthetic counterpart via T2V models. This one-to-one mapping aims to control for high-level semantic variables: by pairing videos with matched scene descriptions, subjects, and actions, we minimize content-based confounds. This design encourages detectors to prioritize learning low-level generative artifacts over semantic correlations, following established protocols

in deepfake detection benchmarks.

We selected five open-source T2V models representing diverse architectures (detailed in Section 2.1): Wan2.1 [49], CogVideoX [54], SkyReels-V2 [7], Self-Forcing [23], and MAGI-1 [1]. This selection balances scale (1.3B to 24B parameters), efficiency (consumer vs. datacenter GPUs), and architectural diversity (standard DiT, expert transformers, autoregressive variants).

After extensive preliminary evaluation, several open-source models were excluded. Generating thousands of videos using OpenSora 2.0 [42], Step-Video-T2V [38], LTX-Video [19], and CausVid [55] revealed consistent severe artifacts, such as malformed anatomy, temporal flickering and physically implausible motion. Such outputs fail to represent the realistic threat posed by near-photorealistic T2V systems that current detection methods must address. Proprietary models (Sora 2 [40], Google VEO 3.1 [16], Kling 2.5 [30]) were also deliberately excluded despite their state-of-the-art quality. These systems embed visible watermarks (trivial detection artifacts) and enforce strict content guardrails preventing unrestricted human-centric generation. Furthermore, their closed-source nature precludes reproducibility through metadata or seed control. Open-source models better represent the realistic threat landscape: publicly accessible, unrestricted, and fully reproducible.

3.2. Structured Prompt Engineering and Validation

Modern T2V models require tuning across multiple parameters to achieve high-fidelity output. Beyond textual prompts describing desired content (*positive prompts*), generation quality depends also on *negative prompts* (to suppress artifacts like "blurry, distorted") and model-specific captioning styles. Furthermore, each model has distinct optimal prompt structures based on its training data distribution [1, 7, 23, 49, 54]. To address these requirements while ensuring semantic consistency and ethical soundness, we developed a two-stage protocol detailed below.

Structured Prompt Generation and Adaptation. Different T2V models are trained with distinct captioning styles, requiring tailored prompts to obtain optimal output quality. Following HunyuanVideo's multi-dimensional framework [28], we employed a Vision-Language Model [56] to generate structured metadata for each source video across seven fields: *short description* (concise summary), *dense description* (detailed actions and camera work), *background* (environment), *style* (aesthetic), *shot type* (cinematography), *lighting*, and *atmosphere* (mood). This unified representation serves as a common source from which we dynamically construct model-specific prompts by selecting and ordering fields according to each generator's training distribution. For instance, CogVideoX [54] uses only four core fields (*dense_description, style, shot_type, background*), while

SkyReels-V2 [7] incorporates all seven fields but prioritizes *style* and *shot_type* first. While prompt structure varies across models, all derive from identical underlying metadata, ensuring semantic consistency. We also augmented baseline negative prompts recommended by model authors through iterative curation, empirically adding keywords to suppress recurring artifacts like stylistic inconsistencies and unwanted text overlays (e.g., "cartoon, watermark").

Manual Prompt Validation Each of the 1,363 structured prompts underwent manual field-by-field validation to verify consistency with source video content and detect potentially sensitive or harmful content. Following manual review, all prompts were subjected to automated screening using a Large Language Model (LLM) [17] to detect subtle sensitive content that might have been missed. The LLM was instructed to flag references to seven thematic categories: violence and warfare, weapons, vulnerable individuals, political figures and institutions, geopolitical references, national symbols with political connotations, and identifiable real persons. Flagged prompts were manually rewritten to neutralize sensitive elements while preserving visual and narrative intent. These iterations continued until all prompts passed both human and automated screening.

3.3. Video Synthesis and Quality Control

Once prompts are validated, we proceed to video generation with careful attention to parameter optimization and output quality. Each T2V model has distinct optimal settings for inference hyperparameters (e.g., classifier-free guidance scale (CFG), diffusion steps, temporal shift [21, 22]), as well as resolution, frame rate, duration, and aspect ratio based on its training data distribution. To ensure each generator operates at peak performance while reflecting real-world deployment scenarios, we developed a comprehensive synthesis protocol combining diversity across temporal, spatial, and format parameters with rigorous manual validation for visual quality and ethical compliance.

Generation Diversity To reflect the heterogeneity of modern synthetic media, we introduce diversity across temporal, spatial, and format parameters. Following each model's recommended optimal settings, we generated videos with durations of $4 - 6$ seconds at frame rates between $8 - 24$ FPS, using resolutions from 480×832 up to 1280×720. Inference parameters (CFG scale, diffusion steps, temporal shift) were set according to author guidelines to maximize output quality [1, 7, 23, 49, 54]. A key distinguishing feature is the systematic aspect ratio diversity. We generated 2,732 landscape videos (16:9, 5:3) and 4,083 portrait videos (3:4, 9:16, 3:5), with near-even splits for models supporting multiple orientations (e.g., SkyReels-V2 [7]: 661 landscape, 702 portrait). This variability en-

Table 1. Overall statistics of the SynthForensics benchmark.

Metric	Value
Unique Synthetic Videos	6,815
Total Video Files (4 versions)	27,260
Total Unique Frames	~550,652
Total Unique Video Duration	~9.5 hours
Landscape Videos (#)	2,732
Portrait Videos (#)	4,083
Resolution Range	480×832 to 1280×720
Frame Rate Range (FPS)	8 to 24
Duration Range (s)	4 to 6

Table 2. Average VBench scores across SynthForensics versions. Metrics: Subject & Background Consistency (temporal stability); Motion Smoothness (fluidity, absence of jitter); Dynamic Degree (motion amount); Aesthetic and Imaging Quality (visual appeal and technical fidelity).

VBench Metric [25]	Raw	Canonical	CRF23	CRF40
Subject Consistency	0.976	0.976	0.976	0.972
Background Consistency	0.960	0.961	0.954	0.961
Motion Smoothness	0.992	0.992	0.993	0.994
Dynamic Degree	0.320	0.320	0.314	0.257
Aesthetic Quality	0.525	0.527	0.515	0.495
Imaging Quality	0.723	0.724	0.724	0.677

sures detectors are tested on fundamental video characteristics rather than overfitting to a single format.

Manual Video Validation Every synthesized video underwent manual inspection for anatomical inconsistencies, rendering errors, temporal artifacts (flickering, discontinuities), semantic coherence with prompts, and ethical compliance. Rejected videos triggered comprehensive refinement: prompt rewriting, negative prompt augmentation with artifact-specific keywords, and generation parameter adjustment (CFG scale, steps, temporal shift). This iterative loop of generation, inspection, refinement, and regeneration repeated until a high-fidelity, coherent, and ethically sound video was accepted. Only videos successfully passing this rigorous validation constitute the final 6,815 samples.

3.4. Dataset Versions, Statistics and Metadata

We provide four versions of each video to facilitate robustness analysis. Raw version is the direct, unprocessed generator output. Canonical version re-encodes each video with uniform parameters (H.264 CRF=0 lossless, YUV420p, BT.709 color space) while preserving original resolutions, neutralizing potential format-specific confounds. CRF23 and CRF40 versions apply progressive compression to Canonical videos to simulate real-world distribution scenarios. Table 1 summarizes the benchmark's diversity. Beyond manual inspection, we objectively quantified dataset quality using VBench [25] automated metrics across all four versions (Table 2). Temporal stability remains consistently high across all compression levels (Subject Consistency > 0.97, Motion Smoothness > 0.99), with negligible differences between Raw and Canonical versions confirming our standardization preserves quality. Compression selectively impacts motion dynamics (Dynamic Degree: -20% at CRF40) and visual fidelity (Imaging Quality: $0.724 \rightarrow 0.677$), while maintaining structural coherence. Finally, we release comprehensive metadata (prompts and inference generation parameters) ensuring reproducibility and enabling research into generation-artifact relationships.

4. Experimental Protocol

Our experimental protocol is designed as a multi-stage investigation to holistically evaluate current detectors against SynthForensics. We begin by quantifying the zero-shot performance gap and robustness of state-of-the-art methods on SynthForensics, analyzing their fragility under compression, controlled real data provenance shifts, and compound distribution shifts. We then investigate dataset learnability through fine-tuning experiments to assess architectural adaptability. Finally, we explore the critical challenge of generalization by training models on a subset of generators and testing on held-out models, while concurrently measuring backward transferability to legacy manipulation-based benchmarks. To enable this evaluation, we selected nine state-of-the-art detectors spanning diverse architectural paradigms (Section 2.3): five frame-level detectors (CFM [37], RECCE [5], ProDet [10], UCF [51], Effort [53]) and four video-level detectors (AltFreezing [50], FTCN [58], GenConViT [11], DFD-FCG [20]).

All detectors were evaluated zero-shot using their publicly available pre-trained weights. Excluding CFM [37] due to unavailable training code, all remaining models were selected for fine-tuning and training-from-scratch experiments to maximize architectural diversity while ensuring reproducible training. Experiments were conducted using official implementations where available, supplemented by the DeepfakeBench [52] framework for reproducible evaluation. We adopt video-level Area Under the Receiver Operating Characteristic Curve (AUC) as primary evaluation metric, providing threshold-independent assessment. For frame-level detectors, video-level predictions were computed by averaging frame-wise predictions.

4.1. Evaluation Datasets

Our experimental protocol leverages SynthForensics and several public datasets to comprehensively assess detector performance. All splits ensure rigorous and reproducible evaluations.

5

Training and Validation Sets. Both derived from raw FF++ [45] official splits paired with SynthForensics counterparts: **SynthForensics-Train** (FF++ [45] train split) and **SynthForensics-Val** (FF++ [45] val split, used for hyperparameter tuning and early stopping).

Primary Evaluation Sets. We designed two tiers of evaluation sets balancing controlled experiments with realistic stress testing.

Tier 1: Controlled Single-Variable Evaluation Sets. To isolate specific failure modes, we constructed two testbeds maintaining our paired-source protocol while varying real data provenance:

- **SF-FF++** (In-domain baseline): FF++ [45] test reals paired with their SynthForensics counterparts, measuring synthetic detection difficulty when real distribution matches training.
- **SF-DFD** (Provenance shift): 363 DFD [14] reals (controlled lab recordings) paired with SynthForensics counterparts, isolating whether detectors rely on FF++ [45] YouTube compression artifacts versus learning true synthetic patterns.

Tier 2: Cross-Domain Stress Evaluation Set. While paired evaluation enables controlled analysis, real-world deployment faces compounded distribution shifts. We therefore construct:

- **SF-CDF** (Compound shift): 178 CDF [32] reals and 178 randomly sampled SynthForensics videos per generator (89 from SF-FF++, 89 from SF-DFD). This deliberately unpaired testbed enables robustness assessment when both real content distribution (celebrity footage vs. YouTube/lab) and synthetic semantic alignment shift simultaneously, simulating realistic worst-case deployment where detectors encounter novel real contexts against synthetic content from unseen semantic prompts.

To ensure fair comparison across compression levels, raw real videos in all Primary Evaluation Sets were re-encoded using the same standardized pipeline applied to synthetic videos (Section 3.4), yielding Canonical, CRF23, and CRF40 versions. Each set is thus available in four matched versions with identical compression conditions.

Legacy Benchmark Sets. To assess backward compatibility and transfer to traditional manipulation-based deepfakes, we evaluate on three benchmarks: **FF++** [45] (official test split), **DFD** [14] (363 reals + ∼3,000 manipulations), and **CDF** [32] (official test set split).

4.2. Evaluation Protocols

We evaluate detectors through three protocols: zero-shot, fine-tuning and training from scratch.

Zero-Shot Evaluation Protocol. This protocol quantifies the performance gap when state-of-the-art detectors encounter purely synthetic video, establishing baseline capabilities and identifying critical fragilities. We conduct two complementary experiments. First, we evaluate all nine detectors on both Legacy Benchmark Sets and Primary Evaluation Sets (Raw versions), directly comparing performance on manipulation-based vs. purely synthetic content. This quantifies the mean performance gap. Second, we evaluate all nine models across the four SF-FF++ versions (Raw, Canonical, CRF23, CRF40) to measure robustness under encoding standardization and progressive compression.

Fine-tuning Protocol. This protocol investigates architectural adaptability to purely synthetic video, quantifying both learning efficacy on SynthForensics and backward compatibility with traditional deepfakes. We fine-tuned eight models on SynthForensics-Train using a conservative protocol designed to preserve pre-trained representations while adapting to synthetic artifacts. Starting from original pre-trained weights on manipulation-based datasets, we employed each model's native optimizer and batch size to maintain architectural consistency. Training used learning rate 1e-5 to prevent catastrophic forgetting, weight decay 1e-4, standard augmentations, maximum 25 epochs, and early stopping (patience 10) based on validation AUC. Fine-tuned models were evaluated on Primary Evaluation Sets to assess SynthForensics learnability via performance gains, and on Legacy Benchmark Sets to measure catastrophic forgetting.

Training from Scratch and Generalization Protocol. This protocol investigates forward generalization to unseen synthetic threats by training on generator subsets, simulating realistic scenarios where new T2V models emerge after detector deployment. We trained eight detectors from scratch on SynthForensics-Train using three generators (Wan2.1 [49], CogVideoX [54], SkyReels-V2 [7]) while holding out Self-Forcing [23] and MAGI-1 [1] as unseen test generators. This split enables measuring In-Domain performance (training generators) versus Out-of-Domain generalization (held-out generators) on Primary Evaluation Sets. MAGI-1 [1] tests cross-architecture robustness via its autoregressive paradigm, while Self-Forcing [23] assesses intra-family generalization and represents the most urgent real-world threat: consumer-grade efficiency enabling unrestricted synthesis on commodity hardware. We trained detectors from scratch, initializing backbones with pretrained weights where available and randomly initializing detection layers, using native optimizers, recommended learning rate schedules, and batch sizes ensuring fair architectural comparison. Training used weight decay 1e-4, standard augmentations, maximum 50 epochs, and early stopping (patience 10) based on validation AUC. Models were evaluated on: (1) Primary Evaluation Sets for forward generalization analysis (In-Domain vs. Out-of-Domain), and (2)

Table 3. Zero-shot performance (Video AUC %) on Legacy Benchmarks (manipulation-based) and Primary Evaluation Sets (SF-FF++, SF-DFD: paired-source; SF-CDF: cross-domain). *Frame-level detector. †Our evaluation, ‡third-party results [9, 53].

Detector	Trained on	Legacy Benchmark Sets			Primary Evaluation Sets			Performance Gap	
		FF++ [45]	DFD [14]	CDF [32]	SF-FF++	SF-DFD	SF-CDF	vs. FF++ [45]	Mean
CFM* [37]	FF++ [45]	99.56	95.21	89.65	81.76	77.69	70.52	−17.80	−18.15
RECCE* [5]	FF++ [45], DFDC [12], CDF [32], WildDeepfake [59]	96.21†	89.10‡	99.94	40.21	44.81	48.00	−56.00	−50.74
ProDet* [10]	FF++ [45]	95.21†	90.10‡	84.48	62.20	49.22	65.31	−33.01	−31.02
UCF* [51]	FF++ [45]	98.61†	94.50	82.40‡	73.16	88.17	74.74	−25.45	−13.15
Effort* [53]	FF++ [45]	96.73†	96.50	95.60	77.82	77.05	55.10	−18.91	−26.29
AltFreezing [50]	FF++ [45]	98.60	98.50	89.50	54.90	75.73	49.83	−43.70	−35.38
FTCN [58]	FF++ [45]	99.70	94.40‡	86.90	50.61	62.78	58.74	−49.09	−36.29
GenConViT [11]	FF++ [45], DFDC [12], TM [8], CDF [32], TIMIT [29]	99.60	99.94†	98.10	87.18	95.24	76.71	−12.42	−12.84
DFD-FCG [20]	FF++ [45]	99.57†	87.38 †	95.00	93.26	84.34	85.11	−6.31	−6.41

Legacy Benchmark Sets for backward transfer to traditional manipulation-based deepfakes.

5. Results and Analysis

This section evaluates detectors through zero-shot assessment and training experiments measuring gaps, compression robustness, learnability and generalization.

5.1. Zero-Shot Evaluation

Performance Gap Analysis. Table 3 reveals systematic performance degradation across all detectors when transitioning from manipulation-based benchmarks to purely synthetic video. The most controlled measure is the FF++ [45] vs. SF-FF++ comparison, where real videos are identical and synthetic content is semantically matched to the training distribution, with drops due solely to synthetic difficulty. We observe a mean performance drop of 29.19 AUC points (averaging individual detector drops from FF++ [45] to SF-FF++). Notably, the most robust foundation model (DFD-FCG [20]) loses 6 points, while reconstruction-based methods like RECCE [5] experience catastrophic failure with a 56 points drop, performing worse than random chance. This consistent collapse across diverse architectures demonstrates that current state-of-the-art detectors are unprepared for artifacts produced by modern T2V models.

Controlled Real-Domain Shift. To assess whether poor performance stems from FF++ [45] real domain overfitting, we evaluate on SF-DFD, which maintains our paired-source protocol while shifting real provenance to controlled lab recordings. Results confirm the challenge lies with synthetic content: performance remains critically low (mean: 72.78% Video AUC), with only three detectors exceeding 80% (UCF [51]: 88.17%, GenConViT [11]: 95.24%, DFD-FCG [20]: 84.34%), while the majority fail substantially, with the lowest performers being RECCE [5] (44.81%),

ProDet [10] (49.22%), and FTCN [58] (62.78%). This demonstrates detector failure on purely synthetic video is independent of FF++ [45] characteristics.

Cross-Domain Stress Test To assess robustness under compounded real-world shifts, we evaluate on SF-CDF, which deliberately combines real content distribution shift (celebrity footage) with unpaired synthetic samples from diverse semantic contexts. Despite this worst-case scenario, catastrophic failure persists (mean: 64.90% Video AUC), with reconstruction methods collapsing (RECCE [5]: 48.00%) and even foundation models degrading severely (DFD-FCG [20]: 85.11%). Results on all Primary Evaluation Sets confirms that detectors consistently struggle with purely synthetic videos, regardless of real data features or semantic similarity.

Robustness to Compression. We evaluated zero-shot performance across SF-FF++ compression levels (Canonical, CRF23, CRF40). Figure 3 shows dramatic degradation: at CRF40, DFD-FCG and GenConViT lose 32 and 34 points respectively, revealing severe fragility under compression.

5.2. Training and Generalization

We investigate dataset learnability through two protocols: fine-tuning to assess adaptability and backward compatibility, and training from scratch to evaluate forward generalization to unseen generators and transfer to traditional manipulation-based deepfakes.

5.2.1. Fine-Tuning Evaluation

Table 4 demonstrates substantial improvement in detecting synthetic videos. We observe a mean gain of 29.13% Video AUC on SF-FF++. The most significant improvement is RECCE [5], leaping from worse-than-random 40.21% to 98.42%. Similarly, AltFreezing [50] improves by 44 points. Even strong DFD-FCG [20] reaches near-perfect 99.03%.
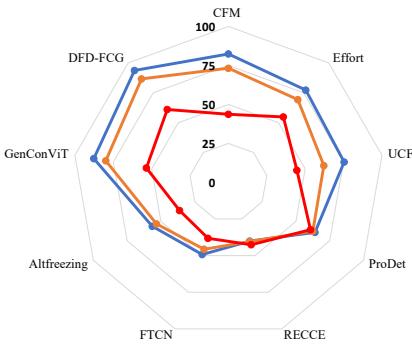
Figure 3. Zero-shot performance (Video AUC %) of state-of-the-art detectors on the SF-FF++ test set across three different versions: (— Canonical), (— CRF23), and (— CRF40).

Table 4. Fine-tuning efficacy: zero-shot vs. fine-tuned performance on SF-FF++ and backward compatibility on FF++. *Frame-level detector.

Detector	Zero-Shot (on SF-FF++)	Fine-Tuned (on SF-FF++)	Gain (Δ)	Backward (on FF++ [45])
RECCE* [5]	40.21	98.42	58.21	56.91
ProDet* [10]	62.20	98.88	36.68	56.77
UCF* [51]	73.16	80.31	7.15	54.45
Effort* [53]	77.82	99.31	21.49	68.16
AltFreezing [50]	54.90	99.11	44.21	64.62
FTCN [58]	50.61	97.54	46.93	55.69
GenConViT [11]	87.18	99.76	12.58	96.31
DFD-FCG [20]	93.26	99.03	5.77	92.47

This proves SynthForensics provides highly effective training signal, adapting even challenged architectures to T2V fakes. Backward compatibility on FF++ [45] reveals a critical trade-off. Robust models like GenConViT [11] maintain high performance (96.31%), indicating no catastrophic forgetting. Conversely, FTCN [58] and ProDet [10] show notable degradation (55.69%, 56.77%), revealing an incompatibility between adapting to modern synthetic artifacts and retaining capability on legacy manipulations.

Table 5. Training from scratch: in-domain, out-of-domain and legacy transfer (mean Video AUC %). *Frame-level detector.

Detector	In-Domain	Out-of-Domain	Legacy Benchmark Sets
RECCE* [5]	99.18	97.64	56.67
ProDet* [10]	96.83	93.57	53.22
UCF* [51]	98.60	96.55	57.84
Effort* [53]	98.91	96.07	61.89
AltFreezing [50]	98.72	98.08	60.69
FTCN [58]	95.55	97.40	55.82
GenConViT [11]	96.01	88.34	52.10
DFD-FCG [20]	86.06	82.79	50.63

5.2.2. Training from Scratch and Generalization

We trained eight models from scratch on a three-generator subset (Wan2.1 [49], CogVideoX [54], SkyReels-V2 [7]), holding out two others (MAGI-1 [1] and Self-Forcing [23])

as unseen test generators. This split enables measuring generalization on Primary Evaluation Sets: In-Domain performance (averaged across the three training generators) versus Out-of-Domain performance (averaged across the two held-out generators). Table 5 demonstrates strong generalization within the synthetic video domain. In-Domain performance reaches 96.23% AUC, confirming SynthForensics provides robust training signal. Out-of-Domain performance remains high at 93.81%, indicating that training on diverse generator subsets enables learning features effective against architecturally novel synthetic threats. However, backward transfer to Legacy Benchmark Sets collapses dramatically (56.11% mean Video AUC), approaching near-random performance. This reveals fundamental incompatibility: manipulation artifacts (blending, warping) and generation artifacts (diffusion fingerprints) represent distinct forensic domains, requiring specialized detection strategies.

6. Conclusion and Discussion

We introduced SynthForensics, the first human-centric benchmark specifically designed for detecting purely synthetic video deepfakes generated by modern Text-to-Video models. Through a paired-source protocol and extensive two-stage human-in-the-loop validation, we constructed a dataset of 6,815 high-quality videos from five architecturally diverse, state-of-the-art open-source generators. Our comprehensive experimental evaluation revealed that current state-of-the-art detectors, despite exceptional performance on traditional manipulation-based benchmarks, are fundamentally unprepared for purely synthetic content. This demonstrates an urgent need for the field to shift attention toward this emerging threat. Training experiments proved that SynthForensics enables effective learning: almost all fine-tuned models achieve near-perfect detection of synthetic video, and models trained from scratch on generator subsets generalize strongly to architecturally novel, held-out threats. However, we uncovered a severe limitation: complete incompatibility between forward generalization to future synthetic content and backward compatibility with legacy manipulation techniques, an essential consideration for developing next-generation detectors.

While SynthForensics represents a significant step forward, several directions could extend its scope. First, although our paired-source protocol enables controlled evaluation by minimizing semantic confounds, the real source videos inherit demographic and content biases from FF++ [45] and DFD [14]. Future iterations could incorporate more diverse sources for broader representation. Second, our focus on text-to-video models addresses the currently dominant synthesis paradigm. While image-to-video generators have recently emerged, they share core architectures and generation processes with T2V systems, differing

primarily in input conditioning mechanisms. This architectural overlap suggests comparable detection challenges, though future work could empirically validate this expectation. Despite these limitations, SynthForensics addresses a critical gap in deepfake detection research and provides the community with a rigorous, reproducible testbed for detection methods against modern generative threats. By releasing the benchmark with comprehensive metadata, we aim to catalyze research toward more robust, generalizable detection systems capable of safeguarding multimedia authenticity in an era of increasingly sophisticated synthetic media.

References

[1] Sand. ai, Hansi Teng, Hongyu Jia, Lei Sun, Lingzhi Li, Maolin Li, et al. MAGI-1: Autoregressive Video Generation at Scale. *arXiv preprint arXiv:2505.13211*, 2025. 3, 4, 6, 8, 2

[2] Joy Battocchio, Stefano Dell'Anna, Andrea Montibeller, and Giulia Boato. Advance Fake Video Detection via Vision Transformers. In *Proceedings of the 2025 ACM Workshop on Information Hiding and Multimedia Security*, page 1–11, New York, NY, USA, 2025. Association for Computing Machinery. 3

[3] Matyas Bohacek and Hany Farid. Human Action CLIPs: Detecting AI-generated Human Motion. *arXiv preprint arXiv:2412.00526*, 2025. 3

[4] Zhixi Cai, Kartik Kuckreja, Shreya Ghosh, Akanksha Chuchra, Muhammad Haris Khan, Usman Tariq, et al. AV-Deepfake1M++: A Large-Scale Audio-Visual Deepfake Benchmark with Real-World Perturbations. In *Proceedings of the 33rd ACM International Conference on Multimedia*, page 13686–13691, New York, NY, USA, 2025. Association for Computing Machinery. 3

[5] Junyi Cao, Chao Ma, Taiping Yao, Shen Chen, Shouhong Ding, and Xiaokang Yang. End-to-End Reconstruction-Classification Learning for Face Forgery Detection. In *Proceedings of the IEEE/CVF Conference on Computer Vision and Pattern Recognition*, pages 4113–4122, 2022. 3, 5, 7, 8, 11

[6] Mirko Casu, Luca Guarnera, Pasquale Caponnetto, and Sebastiano Battiato. GenAI mirage: The impostor bias and the deepfake detection challenge in the era of artificial illusions. *Forensic Science International: Digital Investigation*, 50:301795, 2024. 2

[7] Guibin Chen, Dixuan Lin, Jiangping Yang, Chunze Lin, Junchen Zhu, Mingyuan Fan, et al. SkyReels-V2: Infinite-length Film Generative Model. *arXiv preprint arXiv:2504.13074*, 2025. 3, 4, 6, 8, 1

[8] Weiling Chen, Sheng Lun Benjamin Chua, Stefan Winkler, and See-Kiong Ng. Trusted Media Challenge Dataset and User Study. In *Proceedings of the 31st ACM International Conference on Information & Knowledge Management*, page 3873–3877, New York, NY, USA, 2022. Association for Computing Machinery. 3, 7

[9] Yize Chen, Zhiyuan Yan, Guangliang Cheng, Kangran Zhao, Siwei Lyu, and Baoyuan Wu. X2-dfd: A framework for explainable and extendable deepfake detection. *arXiv preprint arXiv:2410.06126*, 2024. 7

[10] Jikang Cheng, Zhiyuan Yan, Ying Zhang, Yuhao Luo, Zhongyuan Wang, and Chen Li. Can We Leave Deepfake Data Behind in Training Deepfake Detector? In *Advances in Neural Information Processing Systems*, pages 21979–21998. Curran Associates, Inc., 2024. 3, 5, 7, 8, 11

[11] Deressa Wodajo Deressa, Hannes Mareen, Peter Lambert, Solomon Atnafu, Zahid Akhtar, and Glenn Van Wallendael. GenConViT: Deepfake Video Detection Using Generative Convolutional Vision Transformer. *Applied Sciences*, 15 (12), 2025. 3, 5, 7, 8, 11

[12] Brian Dolhansky, Joanna Bitton, Ben Pflaum, Jikuo Lu, Russ Howes, Menglin Wang, et al. The DeepFake Detection Challenge (DFDC) Dataset. *arXiv preprint arXiv:2006.07397*, 2020. 2, 3, 7

[13] Alexey Dosovitskiy. An image is worth 16x16 words: Transformers for image recognition at scale. *arXiv preprint arXiv:2010.11929*, 2020. 3

[14] Nick Dufour and Andrew Gully. Contributing Data to Deepfake Detection Research. https://ai.googleblog.com/2019/09/contributing-data-to-deepfake-detection.html, 2019. Accessed: 2025-11-05. 3, 6, 7, 8

[15] Ian J. Goodfellow, Jean Pouget-Abadie, Mehdi Mirza, Bing Xu, David Warde-Farley, Sherjil Ozair, Aaron Courville, and Yoshua Bengio. Generative Adversarial Nets. In *Advances in Neural Information Processing Systems*. Curran Associates, Inc., 2014. 2

[16] Google. New Veo Updates and More AI Progress in Video and Audio. https://blog.google/technology/ai/veo-updates-flow/, 2024. Accessed: 2025-11-05. 2, 4

[17] Aaron Grattafiori, Abhimanyu Dubey, Abhinav Jauhri, Abhinav Pandey, Abhishek Kadian, Ahmad Al-Dahle, et al. The Llama 3 Herd of Models. *arXiv preprint arXiv:2407.21783*, 2024. 4, 3

[18] Luca Guarnera, Oliver Giudice, and Sebastiano Battiato. Level up the deepfake detection: a method to effectively discriminate images generated by gan architectures and diffusion models. In *Intelligent Systems Conference*, pages 615–625. Springer, 2024. 2

[19] Yoav HaCohen, Nisan Chiprut, Benny Brazowski, Daniel Shalem, Dudu Moshe, Eitan Richardson, et al. LTX-Video: Realtime Video Latent Diffusion. *arXiv preprint arXiv:2501.00103*, 2024. 2, 4, 3

[20] Yue-Hua Han, Tai-Ming Huang, Kai-Lung Hua, and Jun-Cheng Chen. Towards More General Video-based Deepfake Detection through Facial Component Guided Adaptation for Foundation Model. In *Proceedings of the IEEE/CVF Conference on Computer Vision and Pattern Recognition*, pages 22995–23005, 2025. 3, 5, 7, 8, 11

[21] Jonathan Ho and Tim Salimans. Classifier-Free Diffusion Guidance. *arXiv preprint arXiv:2207.12598*, 2022. 4

[22] Jonathan Ho, Ajay Jain, and Pieter Abbeel. Denoising Diffusion Probabilistic Models. In *Advances in Neural Information Processing Systems*, pages 6840–6851. Curran Associates, Inc., 2020. 2, 4

[23] Xun Huang, Zhengqi Li, Guande He, Mingyuan Zhou, and Eli Shechtman. Self Forcing: Bridging the Train-Test Gap in Autoregressive Video Diffusion. *arXiv preprint arXiv:2506.08009*, 2025. 3, 4, 6, 8, 2

[24] Xun Huang, Zhengqi Li, Guande He, Mingyuan Zhou, and Eli Shechtman. Self-Forcing: Official Implementation. https://github.com/guandeh17/Self-Forcing, 2025. Accessed: 2025-11-09. 2, 3, 5

[25] Ziqi Huang, Yinan He, Jiashuo Yu, Fan Zhang, Chenyang Si, Yuming Jiang, et al. VBench: Comprehensive Benchmark Suite for Video Generative Models. In *Proceedings of the IEEE/CVF Conference on Computer Vision and Pattern Recognition*, pages 21807–21818, 2024. 5, 9

[26] Liming Jiang, Ren Li, Wayne Wu, Chen Qian, and Chen Change Loy. DeeperForensics-1.0: A Large-Scale Dataset for Real-World Face Forgery Detection. In *Proceedings of the IEEE/CVF Conference on Computer Vision and Pattern Recognition*, 2020. 3

[27] Tero Karras, Miika Aittala, Timo Aila, and Samuli Laine. Elucidating the design space of diffusion-based generative models. *Advances in neural information processing systems*, 35:26565–26577, 2022. 4

[28] Weijie Kong, Qi Tian, Zijian Zhang, Rox Min, Zuozhuo Dai, Jin Zhou, et al. HunyuanVideo: A Systematic Framework For Large Video Generative Models. *arXiv preprint arXiv:2412.03603*, 2025. 2, 4, 3

[29] Pavel Korshunov and Sebastien Marcel. DeepFakes: a New Threat to Face Recognition? Assessment and Detection. *arXiv preprint arXiv:1812.08685*, 2018. 3, 7

[30] Kuaishou Technology. Kling. https://klingai.com/global/, 2024. Accessed: 2025-11-05. 2, 4

[31] Rohit Kundu, Hao Xiong, Vishal Mohanty, Athula Balachandran, and Amit K. Roy-Chowdhury. Towards a Universal Synthetic Video Detector: From Face or Background Manipulations to Fully AI-Generated Content. In *Proceedings of the IEEE/CVF Conference on Computer Vision and Pattern Recognition*, pages 28050–28060, 2025. 2

[32] Yuezun Li, Xin Yang, Pu Sun, Honggang Qi, and Siwei Lyu. Celeb-DF: A Large-Scale Challenging Dataset for DeepFake Forensics. In *Proceedings of the IEEE/CVF Conference on Computer Vision and Pattern Recognition*, 2020. 2, 3, 6, 7

[33] Yuezun Li, Delong Zhu, Xinjie Cui, and Siwei Lyu. Celeb-DF++: A Large-scale Challenging Video DeepFake Benchmark for Generalizable Forensics. *arXiv preprint arXiv:2507.18015*, 2025. 3

[34] Yaron Lipman, Ricky TQ Chen, Heli Ben-Hamu, Maximilian Nickel, and Matt Le. Flow matching for generative modeling. *arXiv preprint arXiv:2210.02747*, 2022. 4

[35] Yaron Lipman, Ricky TQ Chen, Heli Ben-Hamu, Maximilian Nickel, and Matt Le. Flow matching for generative modeling. In *11th International Conference on Learning Representations, ICLR 2023*, 2023. 2

[36] Runtao Liu, Haoyu Wu, Ziqiang Zheng, Chen Wei, Yingqing He, Renjie Pi, and Qifeng Chen. Videodpo: Omni-preference alignment for video diffusion generation. In *Proceedings of the Computer Vision and Pattern Recognition Conference*, pages 8009–8019, 2025. 2

[37] Anwei Luo, Chenqi Kong, Jiwu Huang, Yongjian Hu, Xiangui Kang, and Alex C. Kot. Beyond the Prior Forgery Knowledge: Mining Critical Clues for General Face Forgery Detection. *IEEE Transactions on Information Forensics and Security*, 19:1168–1182, 2024. 3, 5, 7, 11

[38] Guoqing Ma, Haoyang Huang, Kun Yan, Liangyu Chen, Nan Duan, Shengming Yin, et al. Step-Video-T2V Technical Report: The Practice, Challenges, and Future of Video Foundation Model. *arXiv preprint arXiv:2502.10248*, 2025. 2, 4, 3

[39] Zhenliang Ni, Qiangyu Yan, Mouxiao Huang, Tianning Yuan, Yehui Tang, Hailin Hu, et al. GenVidBench: A Challenging Benchmark for Detecting AI-Generated Video. *arXiv preprint arXiv:2501.11340*, 2025. 3

[40] OpenAI. Sora 2. https://openai.com/index/sora-2/, 2024. Accessed: 2025-11-05. 2, 4

[41] William Peebles and Saining Xie. Scalable Diffusion Models with Transformers. In *Proceedings of the IEEE/CVF International Conference on Computer Vision*, pages 4195–4205, 2023. 2

[42] Xiangyu Peng, Zangwei Zheng, Chenhui Shen, Tom Young, Xinying Guo, Binluo Wang, et al. Open-Sora 2.0: Training a Commercial-Level Video Generation Model in $200k. *arXiv preprint arXiv:2503.09642*, 2025. 2, 4, 3

[43] Andre Rochow, Max Schwarz, and Sven Behnke. FSRT: Facial Scene Representation Transformer for Face Reenactment from Factorized Appearance Head-pose and Facial Expression Features. In *Proceedings of the IEEE/CVF Conference on Computer Vision and Pattern Recognition*, pages 7716–7726, 2024. 2

[44] Olaf Ronneberger, Philipp Fischer, and Thomas Brox. U-net: Convolutional networks for biomedical image segmentation. In *International Conference on Medical image computing and computer-assisted intervention*, pages 234–241. Springer, 2015. 2

[45] Andreas Rossler, Davide Cozzolino, Luisa Verdoliva, Christian Riess, Justus Thies, and Matthias Niessner. FaceForensics++: Learning to Detect Manipulated Facial Images. In *Proceedings of the IEEE/CVF International Conference on Computer Vision*, 2019. 2, 3, 6, 7, 8

[46] Kaede Shiohara, Xingchao Yang, and Takafumi Taketomi. BlendFace: Re-designing Identity Encoders for Face-Swapping. In *Proceedings of the IEEE/CVF International Conference on Computer Vision*, pages 7634–7644, 2023. 2

[47] Jiaming Song, Chenlin Meng, and Stefano Ermon. Denoising diffusion implicit models. *arXiv preprint arXiv:2010.02502*, 2020. 4

[48] Ashish Vaswani, Noam Shazeer, Niki Parmar, Jakob Uszkoreit, Llion Jones, Aidan N Gomez, Łukasz Kaiser, and Illia Polosukhin. Attention is all you need. *Advances in neural information processing systems*, 30, 2017. 2

[49] Team Wan, Ang Wang, Baole Ai, Bin Wen, Chaojie Mao, Chen-Wei Xie, et al. Wan: Open and Advanced Large-Scale

Video Generative Models. *arXiv preprint arXiv:2503.20314*, 2025. 2, 4, 6, 8, 1, 3

[50] Zhendong Wang, Jianmin Bao, Wengang Zhou, Weilun Wang, and Houqiang Li. AltFreezing for More General Video Face Forgery Detection. In *Proceedings of the IEEE/CVF Conference on Computer Vision and Pattern Recognition*, pages 4129–4138, 2023. 3, 5, 7, 8, 11

[51] Zhiyuan Yan, Yong Zhang, Yanbo Fan, and Baoyuan Wu. UCF: Uncovering Common Features for Generalizable Deepfake Detection. In *Proceedings of the IEEE/CVF International Conference on Computer Vision*, pages 22412–22423, 2023. 3, 5, 7, 8, 11

[52] Zhiyuan Yan, Yong Zhang, Xinhang Yuan, Siwei Lyu, and Baoyuan Wu. DeepfakeBench: A Comprehensive Benchmark of Deepfake Detection. In *Advances in Neural Information Processing Systems*, pages 4534–4565. Curran Associates, Inc., 2023. 5

[53] Zhiyuan Yan, Jiangming Wang, Peng Jin, Ke-Yue Zhang, Chengchun Liu, Shen Chen, et al. Orthogonal Subspace Decomposition for Generalizable AI-Generated Image Detection. In *Forty-second International Conference on Machine Learning*, 2025. 3, 5, 7, 8, 11

[54] Zhuoyi Yang, Jiayan Teng, Wendi Zheng, Ming Ding, Shiyu Huang, Jiazheng Xu, et al. CogVideoX: Text-to-Video Diffusion Models with An Expert Transformer. *arXiv preprint arXiv:2408.06072*, 2025. 2, 4, 6, 8, 3

[55] Tianwei Yin, Qiang Zhang, Richard Zhang, William T. Freeman, Fredo Durand, Eli Shechtman, and Xun Huang. From Slow Bidirectional to Fast Autoregressive Video Diffusion Models. In *Proceedings of the IEEE/CVF Conference on Computer Vision and Pattern Recognition*, pages 22963–22974, 2025. 2, 4, 3

[56] Boqiang Zhang, Kehan Li, Zesen Cheng, Zhiqiang Hu, Yuqian Yuan, Guanzheng Chen, et al. VideoLLaMA 3: Frontier Multimodal Foundation Models for Image and Video Understanding. *arXiv preprint arXiv:2501.13106*, 2025. 4, 1, 2, 3

[57] Wenxuan Zhang, Xiaodong Cun, Xuan Wang, Yong Zhang, Xi Shen, Yu Guo, et al. SadTalker: Learning Realistic 3D Motion Coefficients for Stylized Audio-Driven Single Image Talking Face Animation. In *Proceedings of the IEEE/CVF Conference on Computer Vision and Pattern Recognition*, pages 8652–8661, 2023. 2

[58] Yinglin Zheng, Jianmin Bao, Dong Chen, Ming Zeng, and Fang Wen. Exploring Temporal Coherence for More General Video Face Forgery Detection. In *Proceedings of the IEEE/CVF International Conference on Computer Vision*, pages 15044–15054, 2021. 3, 5, 7, 8, 11

[59] Bojia Zi, Minghao Chang, Jingjing Chen, Xingjun Ma, and Yu-Gang Jiang. WildDeepfake: A Challenging Real-World Dataset for Deepfake Detection. In *Proceedings of the 28th ACM International Conference on Multimedia*, page 2382–2390, New York, NY, USA, 2020. Association for Computing Machinery. 3, 7

SynthForensics: A Multi-Generator Benchmark for Detecting Synthetic Video Deepfakes

Supplementary Material

7. Technical Appendices Overview

This document presents the technical implementation details and granular experimental analysis supporting the SynthForensics benchmark. The document is organized as follows:

- Section 8 details the structured prompt generation and adaptation process, including the exact system instructions used for semantic alignment and automated safety screening. It reports the model selection protocol via quantitative rejection rate analysis and qualitative failure comparisons, alongside a qualitative gallery demonstrating the semantic and visual fidelity of the final dataset. Furthermore, it provides the inference hyperparameters for every generator, the computational infrastructure specifications, the iterative human-in-the-loop refinement protocols, and a breakdown of dataset statistics and quality metrics.

- Section 9 aggregates the evaluation protocols and results. It defines the frame sampling strategies and performance metrics used to standardize the assessment. Subsequently, it provides granular performance breakdowns, stratified by individual generator, covering the Zero-Shot, Fine-Tuning, and Training from Scratch evaluation scenarios.

8. The SynthForensics Benchmark: Extended Details

This section presents the technical specifications and protocols governing the construction of the SynthForensics benchmark. We first detail the structured prompt generation pipeline, including the system instructions for semantic alignment and the negative prompt optimization strategies. Subsequently, we describe the validation process involving human review and automated safety screening. We then report the model selection criteria based on quantitative rejection rates, followed by the exact inference configurations and computational infrastructure. Finally, we outline the video quality control protocols, provide a qualitative verification of the generated outputs, and present the dataset statistics, including quality metrics and metadata specifications.

8.1. Structured Prompt Generation and Adaptation Details

Our prompting strategy addresses a critical challenge in multi-generator benchmarking: architecture-specific prompt alignment. The five generative models selected for SynthForensics, Wan2.1 [49], SkyReels-V2 [7], Self-

```
System Instruction:  You are a specialized assistant for advanced video analysis.  Your task is to
provide structured captions in JSON format for real videos.  Follow the guidelines below carefully
to produce accurate, detailed, and multidimensional descriptions.
Structured Caption Format:
For each analyzed video, you must generate a structured caption in JSON format that includes the
following components:
{    "short_description":  "A brief description that captures the main essence of the scene in 1-2
sentences",
    "dense_description":  "A comprehensive narrative of the scene.  Describe the subject's
appearance, their specific actions, and interactions",
    "background":  "Detailed description of the environment in which the subject is situated,
including fixed and mobile elements",
    "style":  "Characterization of the video style (e.g., documentary, cinematic, realistic, sci-fi,
etc.)",
    "shot_type":  "Identification of framing and camera dynamics.  Include shot size (e.g., close-up)
and movement type (e.g., pan, tilt)",
    "lighting":  "Description of the lighting conditions in the video (e.g., natural light,
artificial, chiaroscuro, backlight, etc.)",
    "atmosphere":  "Description of the video atmosphere (e.g., cozy, tense, mysterious, serene,
etc.)" }
```

Figure 4. The exact System Prompt utilized with VideoLLaMA 3 [56] to extract the structured positive prompts that guide the synthetic video generation. The schema enforces a 7-field decomposition to ensure separation between aesthetic, semantic, and technical video attributes.

Forcing [23], CogVideoX [54], and MAGI-1 [1], are trained on distinct captioning distributions (e.g., SkyReels-V2 favors cinematic descriptors at the start, while Wan2.1 prioritizes action verbs). A static, monolithic caption would fail to elicit optimal performance across all models. To address these diverse requirements while ensuring semantic consistency and high visual fidelity, we developed a comprehensive two-stage protocol covering both positive and negative conditioning.

8.1.1. Positive Prompt Construction

To ensure semantic consistency, we focused primarily on establishing a robust pipeline for *positive prompt* construction. We adopted a semantic decomposition strategy inspired by HunyuanVideo [28]. Instead of relying on a single unstructured caption, we employed the Vision-Language Model (VLM) VideoLLaMA 3 [56] to extract a unified set of seven semantic fields from each source video:

- **Short Description**: A concise synopsis summarizing the primary subject and spatial context in 1-2 sentences, used for high-level semantic anchoring.
- **Dense Description**: The comprehensive narrative layer of the prompt. It intertwines fine-grained details of the subject's appearance and specific actions with dynamic camera maneuvers (e.g., tracking shots, pans), ensuring that motion is semantically coupled with the visual content.
- **Background**: A dedicated description of the environment in which the subject is situated. This field isolates fixed and mobile environmental elements to maintain depth consistency and prevent subject-background bleeding.
- **Style**: Specifies the visual aesthetic or media genre (e.g., "Documentary", "Cinematic", "News Broadcast"), enforcing stylistic coherence with the source distribution.
- **Shot Type**: Identifies the camera's perspective and dynamics. It combines the framing size (e.g., "Aerial shot", "Close-up", "Medium shot") with specific camera movement descriptors (e.g., "Pan", "Zoom", "Static shot") to

Table 6. Model-specific prompt structures. The fields, derived from the unified metadata, were ordered and combined to align with each generator's optimal input format.

Model	Field Composition and Order
Wan2.1 & Self-Forcing	style, shot_type, short_description, dense_description, background, lighting, atmosphere
SkyReels-V2	dense_description, style, shot_type, background, atmosphere, lighting
Magi-1	short_description, dense_description, background, style, shot_type, lighting, atmosphere
CogVideoX	dense_description, style, shot_type, background

```
{
  "short_description": "A news anchor is sitting
      in a studio, ready to deliver the news.",
  "dense_description": "The video starts with a
      news anchor seated in a chair. She is
      wearing a pink blazer over a black top and
      has shoulder-length dark hair. The
      background features a blue and white
      backdrop with a window showing a blue sky.
      There are text overlays on the screen
      indicating weather information and other
      news updates.",
  "background": "The background includes a blue
      and white curtain with a window that shows
      a blue sky. There is also a graphic overlay
       with text in Chinese characters.",
  "style": "Realistic, News Broadcast",
  "shot_type": "Medium shot, static camera",
  "lighting": "Artificial, bright studio lighting
      ",
  "atmosphere": "Professional"
}
```

Figure 5. Representative example of the raw structured metadata extracted from a source video.

fully characterize the cinematographer's visual approach.
- **Lighting**: details the illumination properties of the scene, capturing specific attributes such as light source direction, hardness (e.g., "Chiaroscuro"), and color temperature.
- **Atmosphere**: Encapsulates the emotional resonance or mood of the video (e.g., "Tense", "Serene", "Mysterious"), guiding the generator's tone beyond mere physical description.

The extraction process was governed by the specific system instruction provided in Figure 4. This prompt enforces a strict JSON schema to ensure high semantic and visual precision. This separation serves two primary functions. First, it enables dynamic reassembly, allowing us to programmatically select and reorder specific field subsets to match the optimal conditioning distribution of each target generator, as detailed in Table 6. Second, it enhances hallucination control; by forcing the VLM to categorize visual information, such as explicitly separating the background from the subject, we minimize the bleeding of context into subject generation. Figure 5 illustrates a representative raw output extracted from the Structured prompt generation pipeline.

8.1.2. Negative Prompt Optimization

While positive prompts guide the semantic content, negative prompts are essential for suppressing generation artifacts and ensuring cleaner outputs. We applied the default negative strings recommended by the authors of each model to ensure they operate correctly. Table 7 lists these baseline prompts. It is worth noting that the distilled version of MAGI-1 does not require negative prompts. As explained in

Table 7. Baseline negative prompts used for each generator.

Model	Baseline Negative Prompt
Wan2.1 & Self-Forcing	`Vibrant colors, overexposed, static, blurry details, artwork, painting, image, still, overall grayish, worst quality, low quality, JPEG compression residue, ugly, incomplete, extra fingers, poorly drawn hands, poorly drawn faces, deformed, disfigured, distorted limbs, fingers fused together, static image, cluttered background, three legs, walking backwards`
SkyReels-V2	`Bright tones, overexposed, static, blurred details, paintings, images, overall gray, worst quality, low quality, JPEG compression residue, ugly, incomplete, extra fingers, poorly drawn hands, poorly drawn faces, deformed, disfigured, misshapen limbs, fused fingers, still picture, messy background, three legs, walking backwards`
MAGI-1	-
CogVideoX	`Overexposed, static, blurred, worst quality, low quality, JPEG compression, ugly, incomplete, extra fingers, poorly drawn, deformed, disfigured, misshapen limbs, fused fingers, messy background, three legs, blurred eyes`

its technical report [1], the guidance signal is baked directly into the model weights during the distillation process.

These baseline prompts were later slightly augmented with specific keywords to remove recurring artifacts found during our manual validation.

8.2. Manual Prompt Validation Details

To ensure the benchmark's semantic fidelity and ethical compliance, every structured prompt underwent a rigorous review process prior to video generation. We employed a team of three independent annotators to validate the 1,363 metadata entries extracted by the VLM [56]. To ensure unbiased assessments, each annotator independently evaluated the prompts against two primary criteria: semantic consistency with the source video (correcting VLM [56] hallucinations) and the absence of overt sensitive or harmful content. If a prompt was flagged by at least one annotator, it triggered a rewriting phase. The rewriting task was assigned to the flagging annotator (or randomly assigned in cases of multiple flags) to neutralize the issue while preserving the original narrative intent. This process followed a strict iterative loop: the revised prompts were re-submitted to the pool and reviewed again until 100% of the dataset passed without flags from any annotator. Of the initial 1,363 prompts, 70 (5.1%) were flagged during manual review and subsequently revised.

Following this human review, we deployed a Large Language Model (LLM) [17] as an additional automated guardrail to detect subtle sensitive content that might have been missed during manual inspection. The LLM applied the system instruction in Figure 6, requiring strict flagging across seven thematic categories. An additional 38 prompts (2.8%) were flagged during automated screening, revised by the annotation team, and revalidated iteratively until all

1,363 prompts passed both human and automated screening.

8.3. Generative Models and Video Synthesis Implementation

This subsection details the selection process applied to candidate architectures and the technical implementation of the final synthesis pipeline.

8.3.1. Quality-Based Model Selection

To construct a benchmark focused on high-fidelity, human-centric synthetic video deepfake detection, we evaluated state-of-the-art open-source T2V architectures capable of generating realistic human subjects. We initially considered ten candidate models: Wan2.1 [49], SkyReels-V2 [7], MAGI-1 [1], Self-Forcing [23], CogVideoX [54], OpenSora 2.0 [42], Step-Video-T2V [38], LTX-Video [19], CausVid [55], and Hunyuan [28]. Hunyuan was immediately excluded due to licensing restrictions that prohibit research use and dataset distribution, leaving nine models for empirical evaluation. For each of the nine candidate models, we generated 1,363 videos using the validated structured prompts (detailed in Section 8.1 and Section 8.2). All videos underwent human quality assessment to identify severe artifacts that compromise photorealistic fidelity: malformed anatomy (e.g., distorted facial features, impossible limb configurations), temporal flickering (frame-to-frame instability), physically implausible motion (unnatural trajectories, violation of kinematic constraints), and static generation (lack of meaningful temporal dynamics or frozen subjects). Videos exhibiting such artifacts were rejected. These quality criteria are essential to ensure the benchmark represents the realistic threat posed by near-photorealistic T2V systems that current detection methods must address,

```
System Instruction:  You are given JSON files containing multiple textual metadata fields
(short_description, dense_description, background, style, shot_type, lighting, atmosphere) that
describe visual content in videos, generated from a captioning model.  Your task is to review
each textual field and identify any occurrence of terms or references related to sensitive, NSFW,
or politically/ethically controversial content.  The keywords and expressions listed below are
provided solely as examples:  you must also identify any term that conveys similar meaning or
carries comparable sensitive implications, including those expressed through slight variations
in spelling, morphology, or wording.

Sensitive content includes, but is not limited to, references to:
• Violence and warfare, such as:  war, aggression, conflict, battle, attack, bomb, explosion,
  missile, drone, airstrike, invasion, homicide, occupation, military, soldier, combat, casualty,
  terrorism, terrorist.
• Weapons, such as:  gun, rifle, pistol, weapon, firearm, shooting, sniper, assault, grenade,
  ammunition.
• Vulnerable individuals and human rights concerns, such as:  child, kid, minor, baby, orphan,
  refugee, displaced, abuse, trafficking, exploitation.
• Political figures and political content, including names like Trump, Putin, or roles and
  institutions such as president, prime minister, government.
• Geopolitical references, such as Ukraine, Russia, Iran, China, Europe.
• Symbolic references to national identity, including the term "flag".  This should only be
  considered sensitive if it explicitly refers to a national or geopolitical entity.
• References to real existing persons, including but not limited to public figures, celebrities,
  politicians, or any known individual.  This includes any explicit naming or implicit mention that
  can identify such a person.
```

Figure 6. The exact System Instruction used for the automated safety screening performed with the LLM [17]. The model acts as an adversarial filter, flagging content across seven specific risk categories to ensure the benchmark remains strictly safe for research distribution.

rather than easily identifiable low-quality outputs.

We established a 30% rejection rate threshold to ensure the benchmark maintains high perceptual quality. This threshold naturally separated candidates into two distinct performance tiers: five models with rejection rates between 1.6% and 13.0%, and four models exceeding 30% (Table 8).

Table 8. Quality assessment results for nine candidate T2V models, sorted by rejection rate. The 30% threshold (heavy line) separates models that meet high-fidelity human-centric generation standards from those with systematic quality limitations.

Model	Rejected Videos	Rejection Rate
Wan2.1	22	1.6%
MAGI-1	47	3.4%
SkyReels-V2	53	3.9%
Self-Forcing	123	9.0%
CogVideoX	177	13.0%
CausVid	430	31.5%
OpenSora 2.0	551	40.4%
Step-Video-T2V	779	57.1%
LTX-Video	896	65.7%

Models surpassing this threshold exhibited systematic generation failures that compromise the benchmark's utility for evaluating detectors on high-quality synthetic human content (see Figure 7 for representative failure cases).

Such systematic quality issues are particularly problematic in human-centric scenarios, where perceptual realism directly impacts real-world applicability.

8.3.2. Selected Models Configuration and Infrastructure

The configuration of the five selected architectures (Wan2.1 [49], SkyReels-V2 [7], MAGI-1 [1], Self-Forcing [23] and CogVideoX [54]) was designed to balance generation diversity with maximal synthesis fidelity. To ensure each model operates at its peak performance, we strictly adhered to the optimal inference settings recommended by the original authors. Consequently, we selected resolution and temporal parameters that align with the native training distributions of each architecture to avoid out-of-distribution artifacts as detailed in Table 9.

The inference process relies on specific noise scheduling algorithms, or schedulers, which determine the trajectory for solving the differential equations during the denoising process [27, 34, 47]. We strictly adhered to the solvers recommended by the original authors (e.g., FlowMatchEuler, DPM++ 2M) to ensure the models operated within their intended numerical stability zones. While most models based on the Diffusion Transformer (DiT) architecture successfully generated content in both landscape and portrait orientations, CogVideoX was restricted to a single aspect ratio. Its 3D Variational Autoencoder (VAE) architecture exhibited significant quality degradation and stability issues when

4

Figure 7. Qualitative Failure Analysis of Excluded Models. We visualize representative artifacts that led to the exclusion of candidate models. OpenSora 2.0 exhibits severe temporal flickering, texture boiling, and frequent static generation with frozen subjects. CausVid suffers from color saturation artifacts and inconsistent background rendering. Step-Video displays severe anatomical deformation ("melting faces") on human subjects. LTX-Video displays severe anatomical deformations, unnatural plastic-like facial textures, and lacks environmental detail.

forced into vertical resolutions during our preliminary validation, necessitating this constraint to maintain the benchmark's high-fidelity standard.

It is important to note that the hyperparameters reported in Table 9 represent the baseline configuration. As part of our quality control protocol, specific generation instances requiring artifact correction underwent targeted parameter fine-tuning, strictly limited to the guidance scale, inference steps, and time shift (where applicable). For full reproducibility, the exact inference parameters are provided in the separate metadata files accompanying each video.

The generation pipeline was executed on a heterogeneous computing cluster. The primary workload for large-scale models (Wan2.1, SkyReels-V2, CogVideoX, MAGI-1) was distributed across three nodes equipped with NVIDIA A100 (80GB) GPUs. Conversely, the Self-Forcing model was specifically deployed on a single NVIDIA RTX 4090 (24GB) node to empirically verify its efficiency on

consumer-grade hardware [24]. The cumulative compute time for this work, encompassing preliminary candidate evaluation, rejected samples, iterative re-generation cycles, and the final production of the dataset, amounted to approximately 2,000 GPU-hours.

8.4. Manual Video Validation and Quality Control

Following the generation phase, every synthesized video underwent a manual inspection to ensure it met the benchmark's standards for high perceptual fidelity. While the selected models offer high baseline quality, they remain subject to stochastic failures inherent to diffusion processes. To curate the final dataset, we employed the same team of three independent annotators described in Section 8.2 to evaluate each generated video. Annotators worked independently without knowledge of the generating model to minimize bias. Each video was assessed against a strict rejection rubric.

Table 9. Baseline generation parameters for the five selected models. Resolutions are reported as Height×Width.

Parameter	Wan2.1	SkyReels-V2	CogVideoX	MAGI-1	Self-Forcing
Scheduler	UniPCMultistep	FlowUniPCMultistep	DPM	FlowMatchEuler	FlowMatch
Guidance (CFG)	5.0	6.0	6.0	1.0	3.0
Inference Steps	50	50	100	16	50
Time Shift	5.0	8.0	-	-	5.0
FPS	16	24	8	24	16
# Frames	81	97	49	96	81
Duration (s)	$\sim$5	$\sim$4	$\sim$6	4	$\sim$5
Res. (Landscape)	480×832	544×960	480×720	720×1280	480×832
Res. (Portrait)	832×480	960×544	-	1280×720	832×480

8.4.1. Inspection Criteria

Annotators were instructed to flag and reject any video exhibiting artifacts in the following categories:

- Anatomical Inconsistencies: Malformed limbs (e.g., polydactyly), facial asymmetry, unnatural eye rendering, or "melting" skin textures during movement.
- Temporal Artifacts: High-frequency flickering (texture boiling), inconsistent background warping, objects disappearing/reappearing without physical cause, or static generation characterized by frozen subjects or lack of meaningful temporal dynamics.
- Rendering Errors: Glitches, black frames, or severe compression-like artifacts inherent to the VAE decoding step.
- Semantic Coherence: Failure to execute the specific action described in the positive prompt (e.g., subject emotion mismatch) or generating camera movements contradicting the metadata.
- Ethical Compliance: Any emergence of unsafe content that might have bypassed the initial prompt screening (e.g., accidental generation of nudity or violence).

8.4.2. Iterative Refinement Protocol

We adopted a conservative validation strategy: any video flagged by at least one annotator triggered rejection and regeneration. Rejected videos underwent targeted correction based on failure mode analysis. We applied a hierarchical correction strategy:

1. Prompt Rewriting: For failures in *Semantic Coherence* or *Ethical Compliance*, the textual prompt was manually rewritten to reduce ambiguity or enforce stricter safety constraints.
2. Negative Prompt Augmentation: For *Anatomical* or *Rendering* artifacts, we augmented the model-specific negative prompts with targeted keywords (e.g., adding "deformed iris" or "glitch") to actively suppress the defect in the next generation pass.
3. Parameter Adjustment: For *Temporal Artifacts* or weak adherence to instructions, we fine-tuned the generation hyperparameters:

- CFG Scale: Adjusted (typically +0.5 to +1.0) to strengthen semantic adherence.
- Inference Steps: Increased (e.g., from 50 to 60) to resolve under-generated details.
- Temporal Shift: Modified to stabilize motion trajectories in models supporting this parameter.

This iterative loop of generation, inspection, and refinement was repeated until a high-fidelity, coherent, and ethically sound video was successfully generated for every sample. Only the videos successfully passing this validation constitute the final 6,815 samples of the benchmark.

8.5. Qualitative Visual Analysis

Figures 8 and 9 illustrate the semantic alignment across two distinct scenarios: a static news anchor studio (Sample A) and a dynamic sports broadcast (Sample B). Despite architectural variances, all five generators correctly interpret complex semantic constraints, such as the pink blazer in Figure 8 or the specific studio layout in Figure 9, demonstrating the robustness of our paired-source protocol.

To inspect fine-grained generative fidelity, Figure 10 provides magnified crops extracted explicitly from the sports broadcast sequence. These details highlight architecture-specific strengths. CogVideoX demonstrates exceptional background stability, maintaining the temporal coherence of the animated screens within the studio (visible across $t = 0$ to $t = 4$) and correctly rendering the "video-within-video" motion without texture boiling. Wan2.1 exhibits superior anatomical integrity during transient facial events, capturing a natural blinking motion ($t = 1$) where the eyelids close and reopen without deforming the iris. MAGI-1 preserves natural kinematic flow during articulated body movement; as the presenter gestures, the high-frequency zebra pattern on her shirt deforms realistically with the body's geometry. Similarly, SkyReels-V2 captures nuanced micro-expressions, maintaining consistent facial landmark geometry during the blinking action at $t = 2$. Finally, Self-Forcing exhibits high-fidelity physics simulation, particularly in hair dynamics, where strands flow naturally over the shoulder without temporal blurring.

Figure 8. Qualitative Comparison (Sample A - News Anchor). Frame sequences ($t = 0$ to $t = 4$) comparing the source video (Row 1) with synthetic outputs. Despite differing architectural priors, all models correctly interpret the prompt (e.g., pink blazer, newsroom setting) while maintaining high identity consistency and stable background rendering over time.
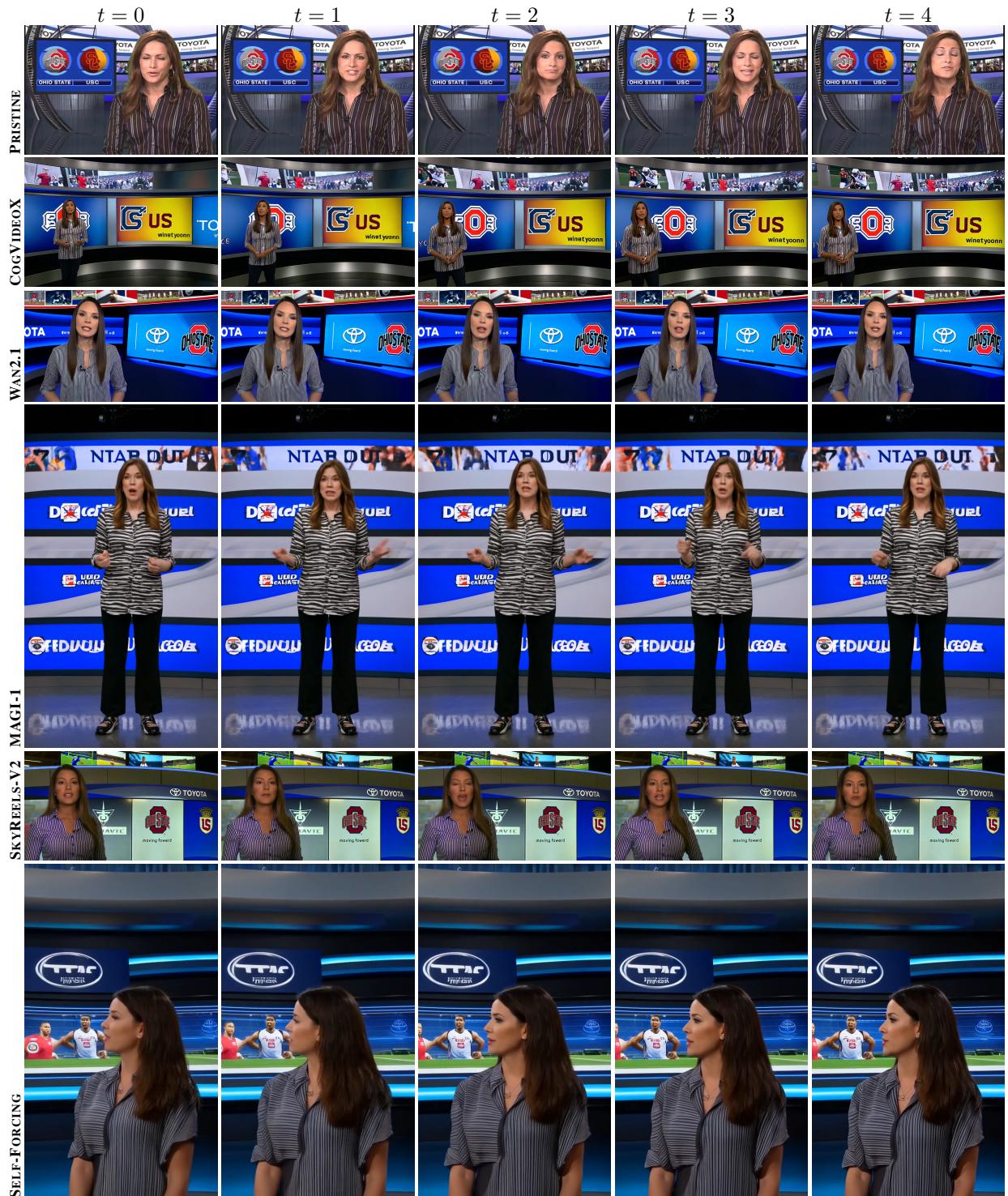
Figure 9. Qualitative Comparison (Sample B - Sports Broadcast). Frame sequences ($t = 0$ to $t = 4$) comparing the source video (Row 1) with synthetic outputs. This scenario tests the models' ability to handle complex backgrounds (screens) and dynamic subject motion.
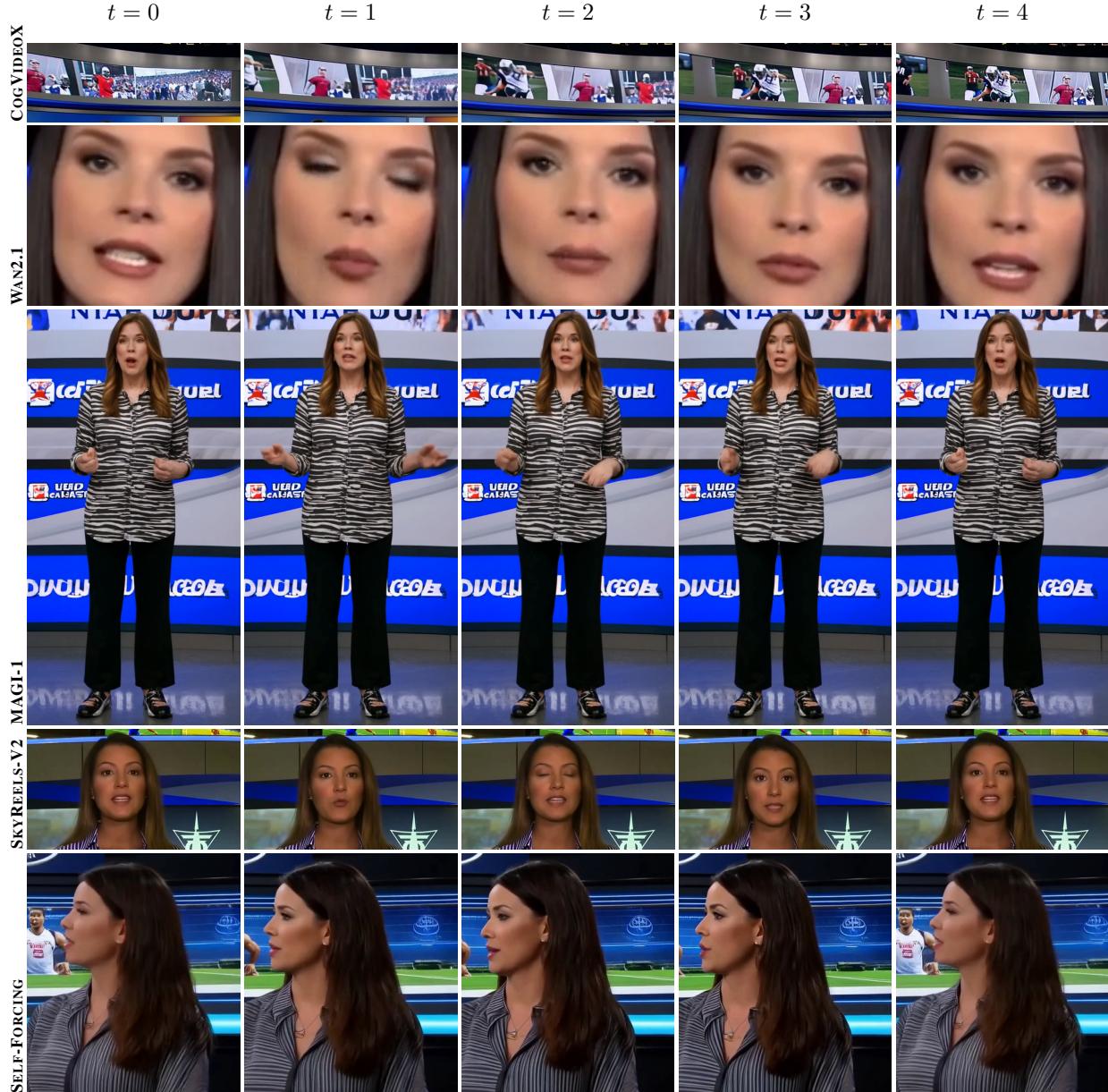
Figure 10. Fine-grained Generation Fidelity Analysis (Sample B - Sports Broadcast). Frame sequences (t = 0 to t = 4) comparing magnified crops extracted from the sports broadcast sequence (Sample B) highlighting architecture-specific strengths. From top to bottom: CogVideoX maintains temporal consistency in animated complex backgrounds; Wan2.1 exhibits high anatomical fidelity in eyes and mouth; MAGI-1 preserves kinematic coherence in body movement; SkyReels-V2 captures nuanced facial expressions; Self-Forcing simulates accurate physics, visible in hair dynamics.

8.6. Dataset Statistics and Metadata

We report per-generator quality metrics, metadata for reproducibility, and aggregate dataset statistics.

8.6.1. Per-Generator Quality Metrics

Table 10 provides a detailed breakdown of VBench [25] scores for each of the five generative models across the four dataset versions (Raw, Canonical, CRF23, CRF40).

An analysis of these metrics reveals distinct performance characteristics among the architectures. CogVideoX consistently exhibits the highest Dynamic Degree (0.486 in Raw), indicating superior motion magnitude, though this comes at a slight cost to Subject Consistency compared to stability-focused models like SkyReels-V2. In terms of robustness, Wan2.1 and Self-Forcing demonstrate remarkable resilience to compression artifacts; even at CRF40, their Imaging

Table 10. Detailed VBench scores per generator across dataset versions. Abbreviations: Subj. Cons.: Subject Consistency; Bg. Cons.: Background Consistency; Mot. Smooth.: Motion Smoothness; Dyn. Deg.: Dynamic Degree; Aest. Qual.: Aesthetic Quality; Img. Qual.: Imaging Quality.

Model	Subj. Cons.	Bg. Cons.	Mot. Smooth.	Dyn. Deg.	Aest. Qual.	Img. Qual.
Raw Version						
Wan2.1	0.978	0.968	0.993	0.327	0.547	0.726
SkyReels-V2	0.983	0.973	0.995	0.329	0.527	0.720
MAGI-1	0.980	0.956	0.994	0.306	0.520	0.721
CogVideoX	0.963	0.951	0.987	0.486	0.489	0.719
Self-Forcing	0.977	0.953	0.994	0.150	0.544	0.729
Mean	*0.976*	*0.960*	*0.992*	*0.320*	*0.525*	*0.723*
Canonical Version						
Wan2.1	0.978	0.968	0.993	0.327	0.546	0.727
SkyReels-V2	0.983	0.973	0.995	0.329	0.527	0.722
MAGI-1	0.980	0.959	0.994	0.306	0.520	0.722
CogVideoX	0.963	0.951	0.986	0.486	0.492	0.721
Self-Forcing	0.977	0.954	0.994	0.150	0.550	0.730
Mean	*0.976*	*0.961*	*0.992*	*0.320*	*0.527*	*0.724*
CRF23 Version						
Wan2.1	0.978	0.954	0.993	0.319	0.526	0.728
SkyReels-V2	0.982	0.967	0.995	0.312	0.512	0.721
MAGI-1	0.980	0.955	0.994	0.305	0.516	0.722
CogVideoX	0.963	0.948	0.987	0.488	0.484	0.720
Self-Forcing	0.977	0.948	0.994	0.148	0.538	0.730
Mean	*0.976*	*0.954*	*0.993*	*0.314*	*0.515*	*0.724*
CRF40 Version						
Wan2.1	0.975	0.962	0.994	0.231	0.500	0.687
SkyReels-V2	0.979	0.970	0.996	0.242	0.490	0.662
MAGI-1	0.977	0.961	0.995	0.258	0.507	0.693
CogVideoX	0.959	0.954	0.988	0.440	0.465	0.675
Self-Forcing	0.973	0.956	0.995	0.115	0.515	0.670
Mean	*0.972*	*0.961*	*0.994*	*0.257*	*0.495*	*0.677*

Quality scores remain competitive, suggesting strong structural integrity in their latent representations. Finally, the negligible score delta between the Raw and Canonical versions across all metrics confirms that our standardization pipeline (re-encoding to H.264 CRF=0, YUV420p, BT.709 color space) successfully normalizes the video format without degrading the generative signal.

8.6.2. Metadata and Reproducibility

To facilitate future research into generation artifacts and ensure full reproducibility, every video in SynthForensics is accompanied by a comprehensive JSON metadata file. This file provides the exact configuration state used to synthesize that specific sample, enabling a deterministic mapping between the real source and the synthetic output.

The metadata fields include:
- `filename`: The identifier linking the synthetic video to its specific Real Source counterpart (FF++ or DFD).
- `width`, `height`: The spatial resolution of the generated video.
- `positive_prompt`: The final structured textual prompt used for conditioning.
- `negative_prompt`: The full negative string (baseline + augmented keywords) used for artifact suppression.
- `video_length`: The total number of frames generated.
- `fps`: The frame rate of the video.
- `cfg`: The specific classifier-free guidance scale used.
- `inference_steps`: The number of denoising steps.
- `time_shift`: The temporal shift parameter (where supported by the architecture).
- `seed`: The random seed used for noise initialization, essential for exact reproduction.

9. Extended Results and Analysis

In this section we present the evaluation methodology designed to execute a fair comparison across diverse detection architectures. We first outline the preprocessing and output standardization steps required to align frame-level and video-level models, and then define the primary metrics used to measure detection efficacy. We extend our evaluation to assess detectors performances across the three evaluation protocols Zero-Shot, Fine-tuning, and Training from scratch.

9.1. Detection Evaluation Metrics

To ensure a comprehensive and reproducible assessment of detector robustness, we adhered to the same preprocessing protocols defined on each evaluated classifier architecture. This approach ensures that every model operates on input data with its specific design requirements consistently. Specifically, we executed the official data preprocessing pipelines encompassing face detection, alignment strategies, cropping margins, and resolution normalization for CFM [37], RECCE [5], ProDet [10], UCF [51], Effort [53], AltFreezing [50], FTCN [58], GenConViT [11], and DFD-FCG [20].

We standardize the output into a single anomaly score $S_V \in [0, 1]$ for each video, representing the aggregate probability that the content is synthetic. The calculation of this score varies based on the detector categories. Frame-level models analyze each sampled frame independently, generating an individual probability score s_i for each frame; in this case, the final video-level score is derived by computing the arithmetic mean of the scores across all K sampled frames as follow:

$$S_V = \frac{1}{K} \sum_{i=1}^{K} s_i \quad (1)$$

Conversely, video-level detectors process the input sequence as a coherent spatiotemporal volume, directly yielding the global score S_V in a single inference pass without requiring post-processing aggregation.

We quantify detection performance using four complementary metrics computed on the ground truth labels $\mathcal{Y}$ (where 0 denotes real and 1 denotes synthetic) and the predicted video-level scores $\mathcal{S}$. The primary metric is the *Area Under the Receiver Operating Characteristic Curve (AUC)*. This metric evaluates the global ranking quality of the detector independent of any specific decision threshold, measuring how well the model separates the positive and negative distributions. The AUC is defined as the area under the ROC curve, computed as the integral of the True Positive Rate (TPR) with respect to the False Positive Rate (FPR):

$$AUC = \int_{0}^{1} \text{TPR}(x) \, dx \quad (2)$$

where x represents the False Positive Rate. An AUC of 50% implies performance equivalent to random guessing, while 100% indicates perfect separability between real and synthetic distributions.

While AUC treats classes symmetrically, we also specifically assess the performance on the synthetic class by reporting the *Average Precision (AP)*. This metric summarizes the Precision-Recall trade-off and is computed as the weighted mean of precisions achieved at each threshold:

$$AP = \sum_{k} (R_k - R_{k-1}) P_k \quad (3)$$

where P_k and R_k represent the Precision and Recall at the k-th threshold, respectively. High AP ensures that the detector is not only separating classes but is also confident in its predictions, penalizing "silent failures" where synthetic videos are ranked lower than real ones.

To evaluate the model's decision capability at a fixed operating point, we measure *Accuracy (Acc)* at a standardized decision threshold $\tau = 0.5$. This metric represents the proportion of correct classifications over the total number of test videos M:

$$Acc = \frac{TP + TN}{M} \quad (4)$$

where TP and TN represent True Positives and True Negatives. Finally, we report the Equal Error Rate (EER), which identifies the specific operating point where the system is balanced, such that the False Acceptance Rate (FAR) is equal to the False Rejection Rate (FRR):

$$EER = \text{FAR}(\tau^*) \quad \text{s.t.} \quad \text{FAR}(\tau^*) = \text{FRR}(\tau^*) \quad (5)$$

A lower EER indicates a more robust equilibrium between the risk of missing deepfakes and the risk of falsely flagging legitimate content.

9.2. Zero-Shot Evaluation Details

We provide a breakdown of detector performance on the three primary evaluation sets: SF-FF++ (In-Domain), SF-DFD (Provenance Shift) and SF-CDF (Compound Shift).

9.2.1. In-Domain Baseline: Analysis on SF-FF++

Table 11. Zero-Shot Video AUC (%). Breakdown by Generator on SF-FF++. *Frame-level detector.

Detector	CogVideoX	MAGI-1	Wan2.1	Self-Forcing	SkyReels-V2	Mean
CFM*	74.61	83,82	79.74	80.31	90.34	81.76
RECCE*	44.14	41.78	35.02	35.61	44.49	40.21
ProDet*	53.59	64.32	64.86	60.90	67.33	62.20
UCF*	58.56	78.26	69.03	83.43	76.54	73.16
Effort*	84.37	80.15	69.00	70.65	84.92	77.82
AltFreezing	59.02	53.12	55.71	48.85	57.82	54.90
FTCN	43.61	44.47	49.64	54.74	60.61	50.61
GenConViT	79.20	82.46	91.16	88.98	94.09	87.18
DFD-FCG	87.18	94.34	94.21	95.33	95.23	93.26

In Table 11, SkyReels-V2 consistently proves to be the least challenging generator; detectors like UCF achieve

respectable performance (76.54% AUC), and DFD-FCG reach near-saturation (95.23%). Conversely, CogVideoX and Wan2.1 represent a significantly higher threat level. For instance, RECCE fails on Wan2.1 (35.02% AUC) and Self-Forcing (35.61% AUC).

Table 12. Zero-Shot Average Precision (AP %). Breakdown on SF-FF++. *Frame-level detector.

Detector	CogVideoX	MAGI-1	Wan2.1	Self-Forcing	SkyReels-V2	Mean
CFM*	70.52	84.37	77.74	78.34	90.53	80.30
RECCE*	46.80	46.04	42.93	41.46	49.33	45.31
ProDet*	53.94	61.30	64.70	60.96	66.76	61.53
UCF*	55.62	70.56	79.22	74.24	86.99	73.33
Effort*	83.19	79.88	70.08	69.20	85.83	77.64
AltFreezing	60.66	57.70	57.56	51.06	62.07	57.81
FTCN	47.37	49.33	53.34	57.75	63.14	54.19
GenConViT	83.24	88.02	93.03	91.28	95.90	90.29
DFD-FCG	87.08	94.74	93.93	94.72	95.89	93.27

Table 12 reveals that precision drops on many detectors on CogVideoX. The AP gap between SkyReels-V2 and CogVideoX is substantial (e.g., for Effort: 84.92% vs 84.37% AUC, but note the drop in other metrics).

Table 13. Zero-Shot Accuracy (Acc %). Breakdown on SF-FF++. Evaluated at threshold 0.5. *Frame-level detector.

Detector	CogVideoX	MAGI-1	Wan2.1	Self-Forcing	SkyReels-V2	Mean
CFM*	50.71	61.79	53.93	54.64	68.93	58.00
RECCE*	45.36	41.07	38.57	37.50	43.57	41.21
ProDet*	51.07	56.79	53.21	54.29	57.86	54.64
UCF*	49.28	54.84	58.03	58.15	58.84	55.83
Effort*	74.10	68.10	62.77	61.71	77.54	68.84
AltFreezing	46.01	46.79	46.28	42.38	46.55	45.60
FTCN	44.15	45.69	49.63	49.41	54.75	48.73
GenConViT	73.91	80.94	87.41	84.70	90.07	83.41
DFD-FCG	74.73	85.00	82.85	83.75	90.94	83.45

In Tables 13 and 14, despite high AUCs, models like GenConViT show an EER of 25.00% on CogVideoX versus 10.00% on SkyReels-V2.

Table 14. Zero-Shot Equal Error Rate (EER %). Breakdown on SF-FF++. Lower values indicate better performance. *Frame-level detector.

Detector	CogVideoX	MAGI-1	Wan2.1	Self-Forcing	SkyReels-V2	Mean
CFM*	31.43	22.86	25.71	25.71	14.29	24.00
RECCE*	53.57	57.86	61.43	60.00	55.00	57.57
ProDet*	45.00	40.00	36.43	42.14	38.57	40.43
UCF*	47.86	35.00	27.14	28.57	24.29	32.57
Effort*	26.43	27.14	34.29	32.14	20.00	28.00
AltFreezing	41.72	47.12	43.88	52.16	43.88	45.75
FTCN	53.96	53.23	50.36	46.40	42.09	49.21
GenConViT	25.00	22.14	15.71	16.43	10.00	17.86
DFD-FCG	22.86	10.00	15.71	11.43	9.29	13.86

9.2.2. Provenance Shift: Analysis on SF-DFD

In Table 15, SkyReels-V2 remains the most detectable source, allowing video-level models like GenConViT to achieve high performance (98.58% AUC). Frame-level detectors exhibit performance degradation (RECCE: 38.62%, ProDet: 46.26%). CogVideoX and Wan2.1 prove more bal-

Table 15. Zero-Shot Video AUC (%). Breakdown by Generator on SF-DFD. *Frame-level detector.

Detector	CogVideoX	MAGI-1	Wan2.1	Self-Forcing	SkyReels-V2	Mean
CFM*	65.27	78.40	79.05	80.35	85.39	77.69
RECCE*	49.59	44.12	44.77	38.62	46.93	44.81
ProDet*	52.38	48.50	49.77	46.26	49.18	49.22
UCF*	78.63	88.42	89.32	93.46	91.03	88.17
Effort*	79.66	72.98	74.74	74.59	83.27	77.05
AltFreezing	73.25	72.91	77.26	79.22	76.03	75.73
FTCN	57.23	55.82	58.10	70.82	71.91	62.78
GenConViT	91.83	95.11	94.51	96.19	98.58	95.24
DFD-FCG	78.39	83.03	84.95	86.87	88.45	84.34

anced but harder overall, dragging even strong baselines like DFD-FCG down to $\sim 78 - 84\%$ AUC.

Table 16. Zero-Shot Average Precision (AP %). Breakdown on SF-DFD. *Frame-level detector.

Detector	CogVideoX	MAGI-1	Wan2.1	Self-Forcing	SkyReels-V2	Mean
CFM*	65.52	76.85	78.57	76.45	84.95	76.47
RECCE*	52.32	46.78	47.04	44.66	50.37	48.23
ProDet*	57.49	52.77	55.05	54.25	55.28	54.97
UCF*	73.32	86.79	88.06	92.97	90.18	86.26
Effort*	76.99	72.78	75.27	75.69	81.59	76.46
AltFreezing	93.90	76.64	77.89	81.23	77.91	81.51
FTCN	60.65	63.43	62.21	75.45	75.98	67.54
GenConViT	90.57	95.16	94.01	96.35	98.40	94.90
DFD-FCG	69.60	77.39	80.62	84.02	86.21	79.57

In Table 16, for Self-Forcing, there is an AP gap: UCF maintains high confidence (92.97% AP), whereas RECCE plummets to 44.66%. Interestingly, even for the strongest model (GenConViT), CogVideoX presents a notable challenge, lowering AP to 90.57% compared to the 98.40% achieved on SkyReels-V2.

Table 17. Zero-Shot Accuracy (Acc %). Breakdown on SF-DFD. Evaluated at threshold 0.5. *Frame-level detector.

Detector	CogVideoX	MAGI-1	Wan2.1	Self-Forcing	SkyReels-V2	Mean
CFM*	52.62	57.02	58.26	55.65	64.05	57.52
RECCE*	48.76	45.32	47.52	42.42	46.69	46.14
ProDet*	49.04	49.59	49.86	48.21	49.45	49.23
UCF*	69.57	75.86	75.23	78.50	75.45	74.92
Effort*	71.96	69.04	70.93	69.45	76.69	71.61
AltFreezing	80.13	54.38	52.99	55.31	53.28	59.22
FTCN	51.28	50.15	50.38	57.68	57.62	53.42
GenConViT	82.68	88.09	87.86	90.30	94.27	88.64
DFD-FCG	68.64	75.29	75.59	78.87	81.09	75.90

In Table 17, detectors like RECCE, ProDet, and FTCN hover near or below 50% accuracy. Conversely, GenConViT achieves its highest accuracy on SkyReels-V2 (94.27%) and Self-Forcing (90.30%).

In Table 18 SkyReels-V2 is effectively detected by GenConViT, which achieves an EER of 5.51%. Self-Forcing follows closely (9.64% EER), but remains an obstacle for other models (RECCE: 57.85% EER). CogVideoX has the highest error rates across the board for top-performing models (GenConViT: 13.77%, DFD-FCG: 29.67%).

Table 18. Zero-Shot Equal Error Rate (EER %). Breakdown on SF-DFD. Lower values indicate better performance. *Frame-level detector.

Detector	CogVideoX	MAGI-1	Wan2.1	Self-Forcing	SkyReels-V2	Mean
CFM*	41.60	28.93	27.55	27.27	21.21	29.31
RECCE*	50.41	53.99	53.72	57.85	51.24	53.44
ProDet*	50.14	52.07	52.34	54.55	52.62	52.34
UCF*	28.65	18.46	18.18	12.95	15.15	18.68
Effort*	28.10	31.40	31.40	30.30	23.42	28.92
AltFreezing	30.06	33.82	29.43	28.18	29.85	30.27
FTCN	43.63	45.51	43.21	33.61	31.94	39.58
GenConViT	13.77	11.29	11.02	9.64	5.51	10.25
DFD-FCG	29.67	22.67	22.33	21.00	20.00	23.13

9.2.3. Compound Shift: Analysis on SF-CDF

In Table 19 SkyReels-V2 remains the most detectable source. Models like GenConViT (89.96%) and DFD-FCG (89.97%) maintain high performance, and even UCF reaches 83.76%. Conversely, CogVideoX and Wan2.1 induce drastic performance drops. GenConViT collapse from $\sim$ 90% on SkyReels-V2 to just 64.87% on CogVideoX. Furthermore, frame-level methods demonstrate limitations on Self-Forcing: RECCE (42.58%) and Effort (45.18%) perform worse than random guessing.

Table 19. Zero-Shot Video AUC (%). Breakdown by Generator on SF-CDF. *Frame-level detector.

Detector	CogVideoX	MAGI-1	Wan2.1	Self-Forcing	SkyReels-V2	Mean
CFM*	61.87	69.37	72.79	78.68	69.87	70.52
RECCE*	51.10	47.21	46.61	42.58	52.51	48.00
ProDet*	62.85	68.45	64.41	69.27	61.57	65.31
UCF*	57.97	73.70	78.90	79.39	83.76	74.74
Effort*	62.29	57.95	45.24	45.18	64.86	55.10
AltFreezing	49.57	46.42	50.84	50.79	51.55	49.83
FTCN	55.50	51.95	54.73	63.67	67.87	58.74
GenConViT	64.87	74.51	78.22	75.98	89.96	76.71
DFD-FCG	76.57	86.01	85.41	87.58	89.97	85.11

In Table 20 a disparity is observed in the transition from SkyReels-V2 to CogVideoX. While GenConViT maintains a robust 89.03% AP on SkyReels-V2, it falls to 59.62% on CogVideoX. Similarly, Effort shows inability to recognize Self-Forcing fakes (32.24% AP).

Table 20. Zero-Shot Average Precision (AP %). Breakdown on SF-CDF. *Frame-level detector.

Detector	CogVideoX	MAGI-1	Wan2.1	Self-Forcing	SkyReels-V2	Mean
CFM*	76.49	85.28	81.52	82.93	89.78	83.20
RECCE*	51.07	48.69	49.03	46.68	53.29	49.75
ProDet*	72.84	75.07	76.47	73.33	78.10	75.16
UCF*	64.07	76.98	82.71	82.13	87.22	78.62
Effort*	47.07	44.97	34.27	32.24	50.88	41.89
AltFreezing	46.07	48.64	48.15	50.00	50.44	48.66
FTCN	52.78	52.39	52.82	63.02	67.62	57.73
GenConViT	59.62	74.63	74.47	80.85	89.03	75.72
DFD-FCG	77.66	87.11	87.37	88.36	91.74	86.45

In Table 21, while models achieve passable accuracy on SkyReels-V2 (e.g., GenConViT: 71.82%, DFD-FCG: 83.28%), they struggle with CogVideoX and Wan2.1. We observe swings of over 15% (e.g., GenConViT drops to

58.73% on CogVideoX). Detectors like AltFreezing hover consistently around 43-45%.

Table 21. Zero-Shot Accuracy (Acc %). Breakdown by Generator on SF-CDF. Evaluated at threshold 0.5. *Frame-level detector.

Detector	CogVideoX	MAGI-1	Wan2.1	Self-Forcing	SkyReels-V2	Mean
CFM*	46.18	54.14	48.73	51.91	59.24	52.04
RECCE*	53.98	50.15	50.74	46.02	53.39	50.86
ProDet*	64.69	67.83	66.08	66.08	67.83	66.50
UCF*	49.16	56.18	56.46	57.30	57.02	55.22
Effort*	59.55	56.55	52.06	50.94	60.67	55.95
AltFreezing	43.14	45.31	44.97	43.67	44.39	44.30
FTCN	51.67	50.71	51.56	56.32	59.02	53.86
GenConViT	58.73	67.06	67.38	68.62	71.82	66.72
DFD-FCG	70.03	78.48	77.27	78.07	83.28	77.43

Finally, in Table 22 SkyReels-V2 allows for relatively low error rates (GenConViT: 14.61% EER). In contrast, CogVideoX proves exceptionally elusive, forcing the Equal Error Rate up to 40.45% for GenConViT and 31.40% for DFD-FCG.

Table 22. Zero-Shot Equal Error Rate (EER %) Breakdown on SF-CDF. Lower values indicate better performance. *Frame-level detector.

Detector	CogVideoX	MAGI-1	Wan2.1	Self-Forcing	SkyReels-V2	Mean
CFM*	39.71	24.26	27.21	28.68	18.38	27.65
RECCE*	49.07	50.31	52.17	52.80	46.58	50.19
ProDet*	34.26	33.33	34.26	37.04	33.33	34.44
UCF*	46.07	33.71	28.09	28.09	25.28	32.25
Effort*	39.33	42.13	52.81	53.93	39.33	45.51
AltFreezing	49.69	53.33	49.69	47.57	48.18	49.69
FTCN	43.93	45.75	45.75	38.48	35.45	41.87
GenConViT	40.45	30.90	28.65	27.53	14.61	28.43
DFD-FCG	31.40	23.26	22.67	21.51	15.70	22.91

9.2.4. Analysis on Robustness to Compression

This section evaluates detector generalization across varying degrees of video compression.

Canonical We initiate the robustness analysis by establishing a performance baseline on the canonical version of SF-FF++. Table 23 details the Zero-Shot Video AUC breakdown. DFD-FCG and GenConViT demonstrate the highest generalization capabilities, achieving mean AUCs of 93.65% and 87.68%, respectively. CFM records a mean of 82.36%, with a peak of 90.53% on SkyReels-V2. Conversely, RECCE and FTCN record lower values, averaging below 50% across the five generators.

Table 24 presents the Average Precision results, reflecting a similar hierarchy. DFD-FCG maintains a mean AP of 93.65%, with GenConViT following at 90.54%. Among frame-level approaches, CFM and UCF record mean APs of 81.34% and 77.75%, respectively. In contrast, other approaches like RECCE and FTCN remain limited to mean APs of 45.39% and 53.31%.

Regarding classification accuracy, Table 25 shows that DFD-FCG and GenConViT surpass 80% mean accuracy.

Table 23. Canonical Compression. Zero-Shot Video AUC (%). Breakdown on SF-FF++ Canonical. *Frame-level detector.

Detector	CogVideoX	MAGI-1	Wan2.1	Self-Forcing	SkyReels-V2	Mean
CFM*	75.96	84.03	80.46	80.81	90.53	82.36
RECCE*	43.99	41.87	35.14	35.41	44.21	40.12
ProDet*	56.05	65.89	66.21	63.11	69.09	64.07
UCF*	58.31	71.32	80.68	80.18	86.26	75.35
Effort*	83.95	79.20	68.34	70.16	84.50	77.23
AltFreezing	60.40	54.46	57.06	50.27	59.16	56.27
FTCN	42.36	43.22	48.38	53.54	59.34	49.37
GenConViT	80.63	83.61	91.60	88.61	93.96	87.68
DFD-FCG	87.81	94.69	94.62	95.68	95.46	93.65

Table 24. Canonical Compression. Zero-Shot Average Precision (AP %). Breakdown on SF-FF++ Canonical. *Frame-level detector.

Detector	CogVideoX	MAGI-1	Wan2.1	Self-Forcing	SkyReels-V2	Mean
CFM*	72.45	84.94	79.09	79.15	91.06	81.34
RECCE*	47.02	46.09	42.91	41.42	49.53	45.39
ProDet*	55.60	61.89	65.05	61.89	67.62	62.41
UCF*	62.05	75.14	83.07	79.16	89.31	77.75
Effort*	82.03	78.57	69.11	68.76	84.71	76.64
AltFreezing	61.97	58.92	58.83	52.27	63.38	59.07
FTCN	46.23	47.95	52.55	57.19	62.62	53.31
GenConViT	84.25	88.68	93.21	90.75	95.80	90.54
DFD-FCG	87.77	95.08	94.33	95.04	96.05	93.65

Table 25. Canonical Compression. Zero-Shot Accuracy (Acc %) Breakdown on SF-FF++ Canonical. Evaluated at threshold 0.5. *Frame-level detector.

Detector	CogVideoX	MAGI-1	Wan2.1	Self-Forcing	SkyReels-V2	Mean
CFM*	50.71	60.36	54.29	54.29	68.93	57.72
RECCE*	45.00	42.14	39.29	37.50	43.21	41.43
ProDet*	52.50	57.86	54.64	56.43	58.93	56.07
UCF*	52.65	58.87	63.08	62.50	62.60	59.94
Effort*	72.20	67.38	62.04	61.48	75.72	67.76
AltFreezing	46.20	46.97	46.47	42.57	46.74	45.79
FTCN	43.41	44.95	48.88	48.63	54.00	47.97
GenConViT	73.19	80.94	87.04	82.84	89.71	82.74
DFD-FCG	75.09	85.71	83.21	84.48	91.30	83.96

Several other detectors, including RECCE, AltFreezing, and FTCN, yield mean accuracy scores between 41% and 48% in this setting.

Table 26. Canonical Compression. Zero-Shot Equal Error Rate (EER %) Breakdown on SF-FF++ Canonical. Lower values indicate better performance. *Frame-level detector.

Detector	CogVideoX	MAGI-1	Wan2.1	Self-Forcing	SkyReels-V2	Mean
CFM*	27.86	23.57	25.71	26.43	16.43	24.00
RECCE*	52.86	57.86	62.14	60.00	55.00	57.57
ProDet*	42.14	37.86	35.71	40.00	37.86	38.71
UCF*	43.65	34.92	25.40	25.40	20.63	30.00
Effort*	24.29	30.00	34.29	33.57	21.43	28.72
AltFreezing	39.21	46.40	44.60	49.28	42.80	44.46
FTCN	55.40	53.59	51.44	47.84	42.81	50.22
GenConViT	23.57	22.14	12.86	16.43	7.86	16.57
DFD-FCG	21.43	11.43	13.57	11.43	12.14	14.00

Finally, Table 26 outlines the Equal Error Rate (EER). DFD-FCG achieves the lowest mean EER of 14.00%, followed by GenConViT at 16.57%. Across the different sources, SkyReels-V2 consistently corresponds to the lowest EER values for the top-performing detectors, specifi-

cally 7.86% for GenConViT and 12.14% for DFD-FCG, while CogVideoX and Wan2.1 result in higher error rates for the majority of the baselines.

CRF23 We extend the analysis to the CRF23 compressed split of SF-FF++, evaluating how the detectors handle quality degradation. Table 27 reports the Zero-Shot Video AUC results. DFD-FCG retains the leading position with a mean AUC of 86.66%, achieving its highest score on MAGI-1 (91.18%). GenConViT follows with a mean of 79.87%. Among the frame-level detectors, CFM demonstrates relative resilience with a mean AUC of 73.22%, while Effort records 69.28%, while RECCE remains at lower performance levels, with mean AUCs of 40.44%.

Table 27. CRF23 Compression. Zero-Shot Video AUC (%). Breakdown on SF-FF++ CRF23. *Frame-level detector.

Detector	CogVideoX	MAGI-1	Wan2.1	Self-Forcing	SkyReels-V2	Mean
CFM*	65.86	80.50	68.06	70.21	81.47	73.22
RECCE*	44.05	41.78	35.78	35.83	44.80	40.44
ProDet*	53.16	65.04	64.98	61.28	68.21	62.53
UCF*	45.67	60.99	64.48	65.01	74.60	62.15
Effort*	79.62	74.75	55.38	62.38	74.28	69.28
AltFreezing	58.57	51.51	53.49	47.43	55.98	53.39
FTCN	39.49	44.20	43.93	49.44	53.20	46.05
GenConViT	72.53	81.73	79.29	79.71	86.10	79.87
DFD-FCG	80.73	91.18	81.59	90.43	89.35	86.66

Table 28. CRF23 Compression. Zero-Shot Average Precision (AP %). Breakdown on SF-FF++ CRF23. *Frame-level detector.

Detector	CogVideoX	MAGI-1	Wan2.1	Self-Forcing	SkyReels-V2	Mean
CFM*	64.45	81.86	66.35	69.82	80.54	72.60
RECCE*	46.85	45.93	43.34	41.45	49.53	45.42
ProDet*	53.19	61.77	64.49	60.54	67.03	61.40
UCF*	50.30	64.03	67.17	63.99	78.24	64.75
Effort*	78.79	75.32	57.07	61.18	75.22	69.52
AltFreezing	60.66	55.27	55.96	50.14	60.72	56.55
FTCN	43.03	48.49	47.92	51.03	56.93	49.48
GenConViT	76.67	18.57	82.66	83.83	88.92	70.13
DFD-FCG	80.98	91.82	82.14	90.13	90.77	87.17

Table 28 details the Average Precision breakdown. DFD-FCG records the highest mean AP at 87.17%. CFM achieves a mean AP of 72.60%, surpassing GenConViT in this specific metric. While GenConViT maintains high precision on SkyReels-V2 (88.92%) and Self-Forcing (83.83%), its mean AP is impacted by a score of 18.57% on the MAGI-1 generator. Effort and UCF record mean APs of 69.52% and 64.75%, respectively.

The accuracy results are presented in Table 29. GenConViT achieves the highest mean accuracy of 76.71%, closely followed by DFD-FCG at 75.46%. Effort records a mean accuracy of 63.06%, outperforming other frame-level baselines such as ProDet (55.78%) and CFM (52.86%). Detectors like RECCE and AltFreezing generally yield accuracy scores below 45%.

Finally, Table 30 shows the Equal Error Rate (EER) analysis. GenConViT records the best overall performance with

Table 29. CRF23 Compression. Zero-Shot Accuracy (Acc %) Breakdown on SF-FF++ CRF23. Evaluated at threshold 0.5. *Frame-level detector.

Detector	CogVideoX	MAGI-1	Wan2.1	Self-Forcing	SkyReels-V2	Mean
CFM*	51.43	56.07	51.79	50.71	54.29	52.86
RECCE*	45.36	42.14	40.36	38.57	44.29	42.14
ProDet*	51.79	58.21	54.64	55.71	58.57	55.78
UCF*	46.59	54.14	55.77	56.42	57.58	54.10
Effort*	70.14	66.67	54.38	56.46	67.63	63.06
AltFreezing	46.19	46.05	46.47	39.45	45.99	44.83
FTCN	43.59	47.52	45.53	48.43	53.07	47.63
GenConViT	65.94	81.29	76.38	77.24	82.72	76.71
DFD-FCG	66.30	81.43	68.98	78.70	81.88	75.46

Table 30. CRF23 Compression. Zero-Shot Equal Error Rate (EER %) Breakdown on SF-FF++ CRF23. Lower values indicate better performance. *Frame-level detector.

Detector	CogVideoX	MAGI-1	Wan2.1	Self-Forcing	SkyReels-V2	Mean
CFM*	37.86	26.43	35.71	34.29	26.43	32.14
RECCE*	53.57	57.86	61.43	57.86	54.29	57.00
ProDet*	47.14	37.86	36.43	40.00	37.86	39.86
UCF*	49.21	41.27	38.89	38.10	32.54	40.00
Effort*	28.57	31.43	47.14	40.71	30.00	35.57
AltFreezing	41.51	49.09	47.67	48.76	45.48	46.50
FTCN	56.31	52.70	54.84	49.82	47.29	52.19
GenConViT	32.86	18.57	25.00	26.43	17.14	24.00
DFD-FCG	27.14	17.14	68.98	17.14	20.71	30.22

a mean EER of 24.00%, showing particular effectiveness on SkyReels-V2 (17.14%). DFD-FCG follows with a mean EER of 30.22%; while it performs well on MAGI-1 and Self-Forcing (17.14%), it records a significantly higher error rate on Wan2.1 (68.98%). CFM and Effort achieve mean EERs of 32.14% and 35.57%, respectively.

CRF40 The robustness analysis includes the evaluation on the heavily compressed SF-FF++ CRF40 split. Table 31 presents the Zero-Shot Video AUC scores. Performance metrics indicate a general decrease across all detectors compared to the lighter compression settings. DFD-FCG and ProDet record the highest stability, achieving mean AUCs of 61.01% and 60.76%, respectively. GenConViT records a mean AUC of 53.44%. Other detectors yield mean values below 45%, with performance on individual generators such as Self-Forcing dropping as low as 24.65% for AltFreezing.

Table 31. CRF40 Compression. Zero-Shot Video AUC (%). Breakdown on SF-FF++ CRF40. *Frame-level detector.

Detector	CogVideoX	MAGI-1	Wan2.1	Self-Forcing	SkyReels-V2	Mean
CFM*	30.41	40.28	46.87	46.64	54.38	43.72
RECCE*	48.20	42.07	38.82	37.79	46.05	42.59
ProDet*	48.91	62.66	63.55	60.68	67.98	60.76
UCF*	40.01	31.41	52.06	48.72	50.90	44.62
Effort*	53.27	59.20	51.78	44.51	64.91	54.73
AltFreezing	40.45	35.50	39.54	24.65	43.74	36.78
FTCN	37.73	38.17	43.77	30.72	47.69	39.62
GenConViT	51.48	51.80	53.67	53.69	56.55	53.44
DFD-FCG	56.68	55.49	63.87	62.78	66.25	61.01

Table 32 displays the Average Precision results. DFD-FCG and ProDet again show comparable performance, with

Table 32. CRF40 Compression. Zero-Shot Average Precision (AP %) Breakdown on SF-FF++ CRF40. *Frame-level detector.

Detector	CogVideoX	MAGI-1	Wan2.1	Self-Forcing	SkyReels-V2	Mean
CFM*	38.81	45.38	47.43	49.21	54.71	47.11
RECCE*	50.52	47.11	45.35	43.25	51.15	47.48
ProDet*	51.40	60.74	62.88	59.96	65.42	60.08
UCF*	45.88	40.71	52.19	49.05	51.61	47.89
Effort*	53.38	60.49	51.86	46.19	65.63	55.51
AltFreezing	45.66	42.58	42.38	31.12	49.28	42.20
FTCN	41.97	44.59	46.71	36.83	52.99	44.62
GenConViT	52.45	55.49	54.62	52.38	56.28	54.24
DFD-FCG	55.75	55.83	63.44	60.77	67.72	60.70

mean APs of 60.70% and 60.08%. Effort and GenConViT follow with 55.51% and 54.24%, respectively. Consistent with previous splits, SkyReels-V2 remains the source yielding the highest precision for the top-performing models, with DFD-FCG achieving 67.72% on this specific generator.

Table 33. CRF40 Compression. Zero-Shot Accuracy (Acc %) Breakdown on SF-FF++ CRF40. Evaluated at threshold 0.5. *Frame-level detector.

Detector	CogVideoX	MAGI-1	Wan2.1	Self-Forcing	SkyReels-V2	Mean
CFM*	46.43	48.93	50.00	51.43	52.50	49.86
RECCE*	46.79	41.79	39.29	40.71	43.57	42.43
ProDet*	46.79	56.07	60.71	55.36	62.14	56.21
UCF*	48.48	43.56	56.20	52.73	52.31	50.66
Effort*	54.15	56.83	52.21	50.93	62.64	55.35
AltFreezing	46.57	44.40	42.94	33.59	45.81	42.66
FTCN	47.31	48.44	53.72	52.34	54.00	51.16
GenConViT	50.72	51.80	54.07	52.06	52.03	52.14
DFD-FCG	53.31	52.69	58.03	55.27	60.73	56.01

The accuracy breakdown in Table 33 shows that most detectors hover near the 50% mark. ProDet and DFD-FCG achieve the highest mean accuracies of 56.21% and 56.01%. Effort and GenConViT record means of 55.35% and 52.14%, while other methods such as RECCE and Alt-Freezing fall below 43% in this setting.

Table 34. CRF40 Compression. Zero-Shot Equal Error Rate (EER %) Breakdown on SF-FF++ CRF40. Lower values indicate better performance. *Frame-level detector.

Detector	CogVideoX	MAGI-1	Wan2.1	Self-Forcing	SkyReels-V2	Mean
CFM*	68.57	57.14	54.29	54.29	47.86	56.43
RECCE*	52.86	56.43	57.14	61.43	52.86	56.14
ProDet*	52.14	40.00	37.86	42.14	35.71	41.57
UCF*	58.73	63.49	49.21	52.38	49.21	54.60
Effort*	51.43	45.71	50.71	58.57	37.86	48.86
AltFreezing	55.11	60.58	56.14	67.93	56.93	59.34
FTCN	58.39	60.22	55.09	64.14	52.92	58.15
GenConViT	50.00	47.86	47.86	47.14	43.57	47.29
DFD-FCG	43.88	46.04	39.57	41.73	37.41	41.73

Finally, Table 34 reports the Equal Error Rates. ProDet and DFD-FCG record the lowest mean EERs of 41.57% and 41.73%. GenConViT follows with a mean EER of 47.29%. The remaining detectors exhibit error rates exceeding 48%, with several baselines recording mean EERs closer to 60%.

9.3. Fine-Tuning Evaluation Details

This section analyzes the performance of detectors after fine-tuning on the SynthForensics-Train split. We evaluate the adapted models across the Pirmary Evaluation Sets and Legacy Benchmark Sets.

9.3.1. Analysis on SF-FF++

Table 35. Fine-Tuning Video AUC (%). Breakdown by Generator on SF-FF++. *Frame-level detector.

Detector	CogVideoX	MAGI-1	Wan2.1	Self-Forcing	SkyReels-V2	Mean
RECCE*	97.24	98.04	98.89	99.29	98.66	98.42
ProDet*	97.96	98.36	98.94	99.74	99.42	98.88
UCF*	78.38	80.14	78.39	78.34	86.27	80.31
Effort*	98.35	99.33	99.64	99.85	99.40	99.31
AltFreezing	98.16	99.61	99.07	99.38	99.35	99.11
FTCN	95.44	98.59	96.84	98.53	98.32	97.54
GenConViT	99.20	99.72	100.00	99.96	99.90	99.76
DFD-FCG	97.88	98.83	99.23	99.87	99.32	99.03

Table 35 shows that most detectors reach high performance levels across all generators. GenConViT achieves 100.00% AUC on Wan2.1 and 99.96% on Self-Forcing. Frame-level models like RECCE and ProDet also report AUCs above 97% for every generator. The exception is UCF, which exhibits lower performance compared to the other models, ranging from 78.34% on Self-Forcing to 86.27% on SkyReels-V2.

Table 36. Fine-Tuning Average Precision (AP %). Breakdown on SF-FF++. *Frame-level detector.

Detector	CogVideoX	MAGI-1	Wan2.1	Self-Forcing	SkyReels-V2	Mean
RECCE*	96.53	97.21	98.29	98.80	98.47	97.86
ProDet*	97.10	97.48	98.26	99.36	98.90	98.22
UCF*	74.89	78.88	77.18	74.40	84.32	77.93
Effort*	97.61	99.04	99.45	99.79	99.11	99.00
AltFreezing	97.54	99.54	98.80	99.24	99.17	98.86
FTCN	94.56	98.52	96.39	98.51	98.28	97.25
GenConViT	99.27	99.72	100.00	99.96	99.91	99.77
DFD-FCG	97.08	98.44	99.04	99.85	99.14	98.71

The AP results in Table 36 largely mirror the AUC trends. Effort maintains AP values above 99% for all five generators. For the UCF detector, a performance gap is observed between generators: it achieves 84.32% AP on SkyReels-V2 but drops to 74.89% on CogVideoX and 74.40% on Self-Forcing.

Table 37. Fine-Tuning Accuracy (Acc %) Breakdown on SF-FF++. Evaluated at threshold 0.5. *Frame-level detector.

Detector	CogVideoX	MAGI-1	Wan2.1	Self-Forcing	SkyReels-V2	Mean
RECCE*	90.42	91.08	92.56	92.82	92.20	91.82
ProDet*	89.69	90.41	90.73	91.57	91.55	90.79
UCF*	56.57	60.39	58.73	59.59	59.07	58.87
Effort*	92.45	94.35	94.41	94.48	94.17	93.97
AltFreezing	94.24	95.77	95.35	95.11	95.53	95.20
FTCN	88.68	91.74	90.33	91.60	91.81	90.83
GenConViT	95.29	96.76	96.67	96.64	96.32	96.34
DFD-FCG	76.87	76.87	76.87	76.87	76.87	76.87

Table 37 evaluates detection accuracy. Frame-level models

such as RECCE and Effort achieve accuracy scores above 91% across all generators. GenConViT records values between 95.29% (CogVideoX) and 96.76% (MAGI-1). DFD-FCG presents a constant accuracy of 76.87% across all subsets, contrasting with its higher AUC scores.

Table 38. Fine-Tuning Equal Error Rate (EER %). Breakdown on SF-FF++. Lower values indicate better performance. *Frame-level detector.

Detector	CogVideoX	MAGI-1	Wan2.1	Self-Forcing	SkyReels-V2	Mean
RECCE*	9.60	8.71	6.99	4.89	6.27	7.29
ProDet*	9.71	8.93	7.88	3.84	5.51	7.17
UCF*	35.84	32.72	34.10	35.06	23.65	32.27
Effort*	7.67	4.91	3.39	2.41	4.10	4.50
AltFreezing	6.11	2.51	3.95	3.23	3.23	3.81
FTCN	10.43	5.03	9.71	5.03	5.75	7.19
GenConViT	5.00	3.57	0.00	0.00	0.00	1.71
DFD-FCG	6.43	4.29	3.57	1.43	2.86	3.72

Table 38 reports the minimum error rates. GenConViT reaches an EER of 0.00% on Wan2.1, Self-Forcing, and SkyReels-V2. Among the generators, CogVideoX consistently yields the highest EERs for several detectors, such as FTCN (10.43%) and ProDet (9.71%), compared to lower values obtained on SkyReels-V2 and Self-Forcing.

9.3.2. Analysis on SF-DFD

Table 39. Fine-Tuning Video AUC (%). Breakdown by Generator on SF-DFD. *Frame-level detector.

Detector	CogVideoX	MAGI-1	Wan2.1	Self-Forcing	SkyReels-V2	Mean
RECCE*	85.69	87.49	93.28	91.04	93.73	90.25
ProDet*	79.68	82.83	88.12	89.96	93.29	86.78
UCF*	72.26	73.76	72.24	77.72	74.55	74.11
Effort*	65.82	63.24	76.48	80.31	72.62	71.69
AltFreezing	95.40	96.42	96.03	96.03	97.65	96.31
FTCN	92.86	97.08	95.05	96.83	97.31	95.83
GenConViT	79.84	81.12	96.69	92.20	98.34	89.64
DFD-FCG	90.54	93.06	96.36	97.04	96.56	94.71

Table 39 highlights performance variations based on the generator. While SkyReels-V2 allows high detection rates (GenConViT: 98.34%, AltFreezing: 97.65%), results drop for CogVideoX. Specifically, GenConViT records 79.84% AUC on CogVideoX, and Effort decreases to 65.82% on the same generator.

Table 40. Fine-Tuning Average Precision (AP %). Breakdown on SF-DFD. *Frame-level detector.

Detector	CogVideoX	MAGI-1	Wan2.1	Self-Forcing	SkyReels-V2	Mean
RECCE*	78.41	81.23	87.18	87.07	87.60	84.30
ProDet*	71.69	72.05	80.20	82.15	82.45	77.71
UCF*	92.40	73.62	71.50	77.53	75.54	78.12
Effort*	56.32	59.53	70.36	80.68	66.45	66.67
AltFreezing	95.70	97.07	96.09	96.71	97.70	96.65
FTCN	92.26	97.34	94.48	96.98	97.35	95.68
GenConViT	73.58	76.97	95.62	92.49	97.95	87.32
DFD-FCG	88.80	93.21	96.31	97.65	96.88	94.57

Table 40 shows a similar trend. Detectors maintain high AP on SkyReels-V2 (GenConViT: 97.95%, FTCN: 97.35%).

Conversely, on CogVideoX, GenConViT's AP falls to 73.58% and Effort's to 56.32%. UCF shows a different pattern, achieving its highest AP on CogVideoX (92.40%) compared to other generators in this split.

Table 41. Fine-Tuning Accuracy (Acc %) Breakdown on SF-DFD. Evaluated at threshold 0.5. *Frame-level detector.

Detector	CogVideoX	MAGI-1	Wan2.1	Self-Forcing	SkyReels-V2	Mean
RECCE*	69.01	70.73	71.14	71.58	71.43	70.78
ProDet*	58.21	60.35	59.44	61.99	60.90	60.18
UCF*	63.22	61.48	63.93	59.70	62.90	62.25
Effort*	46.40	48.78	48.16	51.07	48.38	48.56
AltFreezing	87.01	88.29	87.26	87.71	89.51	87.96
FTCN	82.72	90.61	85.74	89.47	90.78	87.86
GenConViT	50.39	54.12	50.32	53.73	50.64	51.84
DFD-FCG	53.21	57.00	56.41	59.27	58.33	56.84

Table 41 reveals discrepancies at the standard threshold. While AltFreezing and FTCN maintain accuracy scores above 82% for all generators, GenConViT drops to the 50 − 54% range across the board (e.g., 50.39% on CogVideoX). Similarly, DFD-FCG records accuracy values between 53% and 59%.

Table 42. Fine-Tuning Equal Error Rate (EER %) Breakdown on SF-DFD. Lower values indicate better performance. *Frame-level detector.

Detector	CogVideoX	MAGI-1	Wan2.1	Self-Forcing	SkyReels-V2	Mean
RECCE*	24.06	23.41	16.80	17.94	16.82	19.81
ProDet*	29.97	28.37	22.80	20.05	18.55	23.95
UCF*	32.51	33.65	34.27	26.47	28.82	31.14
Effort*	40.07	42.32	31.98	28.21	35.54	35.62
AltFreezing	10.43	9.39	10.22	9.39	6.88	9.26
FTCN	13.98	9.18	12.52	10.02	9.39	11.02
GenConViT	28.10	27.00	9.37	16.80	5.79	17.41
DFD-FCG	17.71	14.93	9.38	8.68	9.03	11.95

Table 42 indicates the error rates achievable by optimizing the threshold. GenConViT shows a large variance between generators: 5.79% EER on SkyReels-V2 versus 28.10% on CogVideoX. Effort records its highest EER on MAGI-1 (42.32%) and CogVideoX (40.07%), while performing better on Self-Forcing (28.21%).

9.3.3. Analysis on SF-CDF

Table 43. Fine-Tuning Video AUC (%). Breakdown by Generator on SF-CDF. *Frame-level detector.

Detector	CogVideoX	MAGI-1	Wan2.1	Self-Forcing	SkyReels-V2	Mean
RECCE*	97.11	98.62	98.97	98.71	99.07	98.50
ProDet*	96.28	96.52	98.15	99.00	99.03	97.80
UCF*	76.26	74.27	76.38	73.86	77.55	75.66
Effort*	96.26	97.21	98.09	98.74	97.73	97.61
AltFreezing	96.36	99.03	97.52	99.16	98.21	98.06
FTCN	86.67	94.43	88.81	94.56	93.36	91.57
GenConViT	96.54	98.40	99.95	99.60	99.53	98.80
DFD-FCG	91.75	94.24	96.93	98.59	96.15	95.53

Table 43 shows that Wan2.1 and Self-Forcing yield high AUC scores for top detectors. GenConViT achieves 99.95% on Wan2.1 and 99.60% on Self-Forcing. CogVideoX

results are generally lower; for instance, FTCN scores 86.67% on CogVideoX compared to 94.56% on Self-Forcing.

Table 44. Fine-Tuning Average Precision (AP %). Breakdown on SF-CDF. *Frame-level detector.

Detector	CogVideoX	MAGI-1	Wan2.1	Self-Forcing	SkyReels-V2	Mean
RECCE*	94.95	96.79	97.62	97.54	97.70	96.92
ProDet*	93.54	93.77	96.41	97.52	96.84	95.62
UCF*	72.89	73.46	72.88	70.51	76.83	73.31
Effort*	93.84	95.96	97.09	98.19	96.23	96.26
AltFreezing	95.96	99.06	97.25	99.04	98.22	97.91
FTCN	80.99	93.55	85.19	92.52	91.68	88.79
GenConViT	96.68	98.25	99.95	99.57	99.59	98.81
DFD-FCG	90.41	94.28	96.62	98.78	96.29	95.28

In Table 44, models like RECCE and AltFreezing consistently exceed 94% AP across all five generators. GenConViT also maintains high precision (> 96%) for all generators. FTCN shows a variation, dropping to 80.99% AP on CogVideoX while maintaining > 91% on SkyReels-V2 and Self-Forcing.

Table 45. Fine-Tuning Accuracy (Acc %). Breakdown on SF-CDF. Evaluated at threshold 0.5. *Frame-level detector.

Detector	CogVideoX	MAGI-1	Wan2.1	Self-Forcing	SkyReels-V2	Mean
RECCE*	89.83	91.39	92.17	91.48	92.22	91.42
ProDet*	82.24	82.46	83.55	83.72	83.81	83.16
UCF*	62.04	62.12	60.97	58.68	62.79	61.32
Effort*	83.80	84.59	84.77	85.34	84.79	84.66
AltFreezing	88.12	90.46	88.79	90.14	90.08	89.52
FTCN	77.42	81.55	78.25	80.78	80.97	79.79
GenConViT	80.42	82.51	81.54	82.09	81.52	81.62
DFD-FCG	50.16	51.52	51.95	53.62	53.35	52.12

Table 45 presents accuracy of all detectors. RECCE and AltFreezing maintain accuracy levels above 88% for all generators. In contrast, DFD-FCG shows accuracy scores in the 50 − 53% range for all subsets. ProDet shows a decline on CogVideoX (82.24%).

Table 46. Fine-Tuning Equal Error Rate (EER %). Breakdown on SF-CDF. Lower values indicate better performance. *Frame-level detector.

Detector	CogVideoX	MAGI-1	Wan2.1	Self-Forcing	SkyReels-V2	Mean
RECCE*	9.76	7.13	6.44	6.61	6.22	7.23
ProDet*	12.25	12.18	9.23	5.99	8.32	9.59
UCF*	34.55	35.78	34.96	36.15	32.29	34.75
Effort*	12.54	10.42	8.59	7.18	10.00	9.75
AltFreezing	10.30	5.15	7.57	4.54	6.36	6.78
FTCN	20.60	12.72	19.09	13.03	14.54	16.00
GenConViT	10.11	6.18	0.56	3.93	1.69	4.49
DFD-FCG	14.53	11.63	11.05	5.23	11.05	10.70

Table 46 reports the lowest error rates. GenConViT achieves 0.56% EER on Wan2.1 and 1.69% on SkyReels-V2, but rises to 10.11% on CogVideoX. A similar pattern is observed for FTCN, which records 20.60% EER on CogVideoX compared to 13.03% on Self-Forcing.

9.3.4. Analysis on Legacy Benchmarks

Following the fine-tuning stage, the backward generalization capabilities are assessed on widely used legacy benchmarks: FaceForensics++ (FF++), DeepFake Detection (DFD), and Celeb-DF (CDF). The quantitative results, summarized in Table 47, reveal a distinct divergence in model behavior.

Table 47. Video AUC (%) on FF++, DFD, CDF. Models finetuned on the proposed dataset and evaluated on traditional benchmarks. Higher values indicate better performance. *Frame-level detector.

Detector	FF++	DFD	CDF	Mean
RECCE*	56.91	55.64	50.30	54.28
ProDet*	56.77	57.58	51.21	55.19
UCF*	54.45	49.89	50.31	51.55
Effort*	68.16	55.91	52.34	58.80
AltFreezing	64.62	52.57	55.82	57.67
FTCN	55.69	54.37	55.37	55.14
GenConViT	96.31	79.11	83.21	86.21
DFD-FCG	92.47	90.52	75.98	86.32

While the majority of detectors (e.g., RECCE, ProDet, FTCN) exhibit performance levels close to random guessing, with mean AUCs ranging from 51.55% to 58.80%, GenConViT and DFD-FCG demonstrate notable robustness, maintaining mean AUCs of 86.21% and 86.32%, respectively. This indicates that for most architectures, the adaptation to the target domain affects the retention of features relevant to legacy artifacts, whereas specific designs preserve better transferability across generation paradigms.

9.4. Training from Scratch and Generalization Details

This section presents the results of detectors trained from scratch solely on a subset of SynthForensics (Wan2.1, CogVideoX, SkyReels-V2). We evaluate detection capabilities on these "In-Domain" generators and measure transferability to "Out-of-Domain" generators (Self-Forcing, MAGI-1) across the three benchmark datasets.

9.4.1. Analysis on SF-FF++

Table 48. Training from Scratch Video AUC (%). Breakdown by Generator on SF-FF++. *Frame-level detector.

Detector	In-Domain				Out-of-Domain		
	CogVideoX	SkyReels-V2	Wan2.1	Mean	Self-Forcing	MAGI-1	Mean
RECCE*	99.45	99.76	99.87	99.90	98.15	99.69	99.03
ProDet*	97.88	99.81	99.64	99.79	96.24	99.11	98.02
UCF*	99.44	99.92	99.97	99.93	98.21	99.78	99.07
Effort*	99.93	99.98	99.99	100.00	99.52	99.97	99.76
AltFreezing	99.58	99.98	99.90	99.96	99.95	99.82	99.96
FTCN	97.15	99.33	98.64	98.87	99.50	98.37	99.19
GenConViT	99.68	99.92	99.97	99.85	98.47	99.86	99.16
DFD-FCG	93.79	92.31	93.12	95.99	89.20	93.07	92.60

Table 48 shows high performance for generators seen during training. Effort and AltFreezing achieve nearly 100%

AUC on CogVideoX, SkyReels-V2, and Wan2.1. Regarding Out-of-Domain generators, MAGI-1 is detected with high efficacy (RECCE: 99.69%, GenConViT: 99.86%). Conversely, Self-Forcing presents a slight performance drop for specific architectures; ProDet records 96.24% on Self-Forcing compared to > 99% on seen generators. DFD-FCG remains an outlier with significantly lower scores (e.g., 89.20% on Self-Forcing).

Table 49. Training from Scratch Average Precision (AP %). Breakdown on SF-FF++. *Frame-level detector.

Detector	In-Domain				Out-of-Domain		
	CogVideoX	SkyReels-V2	Wan2.1	Mean	Self-Forcing	MAGI-1	Mean
RECCE*	99.13	99.65	99.78	99.83	97.83	99.52	98.83
ProDet*	97.31	99.64	99.27	99.34	95.51	98.74	97.43
UCF*	99.17	99.72	99.77	99.73	97.69	99.55	98.71
Effort*	99.79	99.94	99.96	99.96	99.23	99.94	99.60
AltFreezing	99.60	99.97	99.89	99.96	99.94	99.82	99.95
FTCN	96.79	99.26	98.57	98.95	99.50	98.21	99.23
GenConViT	99.62	99.92	99.96	99.83	98.25	99.83	99.04
DFD-FCG	92.80	91.52	93.35	95.57	87.31	92.56	91.44

Table 49 indicates that precision tracks closely with AUC. Detectors maintain > 99% AP on Wan2.1 and SkyReels-V2. For the unseen generators, MAGI-1 is consistently ranked with high precision (Effort: 99.90%), while Self-Forcing causes a noticeable reduction in confidence for ProDet (95.51%) and UCF (97.69%) compared to their In-Domain averages.

Table 50. Training from Scratch Accuracy (Acc %). Breakdown on SF-FF++. Evaluated at threshold 0.5. *Frame-level detector.

Detector	In-Domain				Out-of-Domain		
	CogVideoX	SkyReels-V2	Wan2.1	Mean	Self-Forcing	MAGI-1	Mean
RECCE*	95.60	96.43	97.14	97.15	92.27	96.39	94.71
ProDet*	82.65	95.07	91.27	94.16	75.27	89.66	84.72
UCF*	94.73	95.96	96.09	95.92	91.23	95.59	93.58
Effort*	98.10	98.90	98.99	98.97	95.25	98.66	97.11
AltFreezing	96.10	96.83	96.84	96.67	96.88	96.59	96.78
FTCN	88.49	96.64	94.98	96.09	97.24	93.37	96.67
GenConViT	98.55	98.16	98.52	98.51	93.17	98.41	95.84
DFD-FCG	50.37	50.37	50.37	50.37	50.00	50.37	50.19

Table 51. Training from Scratch Equal Error Rate (EER %). Breakdown on SF-FF++. Lower values indicate better performance. *Frame-level detector.

Detector	In-Domain				Out-of-Domain		
	CogVideoX	SkyReels-V2	Wan2.1	Mean	Self-Forcing	MAGI-1	Mean
RECCE*	4.33	3.21	2.12	1.83	7.75	3.22	4.79
ProDet*	8.15	3.41	4.84	3.77	11.39	5.47	7.58
UCF*	4.60	2.05	1.76	1.92	8.71	2.80	5.32
Effort*	1.96	0.80	0.80	0.62	3.92	1.19	2.27
AltFreezing	2.87	0.71	1.79	1.07	1.07	1.79	1.07
FTCN	7.19	3.23	3.95	3.95	2.87	4.79	3.41
GenConViT	1.43	1.43	0.71	1.43	4.29	1.19	2.86
DFD-FCG	12.86	15.71	15.71	9.29	18.57	14.76	13.93

Table 50 reveals that while seen generators generally allow for > 95% accuracy, disparities emerge with unseen ones. ProDet shows a significant gap: 95.07% accuracy on SkyReels-V2 (In-Domain) versus 75.27% on Self-Forcing (Out-of-Domain). GenConViT maintains stability on MAGI-1 (98.41%) but drops to 93.17% on Self-

Forcing. DFD-FCG exhibits an accuracy of $\sim 50\%$ across all columns.

Table 51 reports minimal error rates for In-Domain generators (e.g., Effort: 0.80% on Wan2.1). For Out-of-Domain testing, Self-Forcing consistently induces higher error rates: ProDet reaches 11.39% and RECCE 7.75%, compared to values typically $< 4\%$ for the seen generators.

9.4.2. Analysis on SF-DFD

Table 52. Training from Scratch Video AUC (%). Breakdown by Generator on SF-DFD. *Frame-level detector.

Detector	In-Domain				Out-of-Domain		
	CogVideoX	SkyReels-V2	Wan2.1	Mean	Self-Forcing	MAGI-1	Mean
RECCE*	96.36	99.28	98.87	97.46	92.29	98.17	94.88
ProDet*	85.79	97.78	93.93	94.98	79.39	92.50	87.19
UCF*	95.09	98.41	97.29	95.76	90.09	96.93	92.93
Effort*	95.37	97.49	97.78	96.25	82.73	96.88	89.49
AltFreezing	97.28	99.36	98.44	95.36	97.54	98.36	96.45
FTCN	94.23	97.55	95.89	96.82	97.37	95.89	97.10
GenConViT	77.49	95.15	93.60	83.70	55.51	88.75	69.91
DFD-FCG	78.39	82.18	83.86	82.67	69.42	81.48	76.05

Table 52 highlights a divergence between detectors. AltFreezing and FTCN maintain high AUC ($> 94\%$) across both In-Domain (CogVideoX) and Out-of-Domain (Self-Forcing) generators. In contrast, GenConViT shows a sharp decline: while it achieves 95.15% on SkyReels-V2, it drops to 77.49% on CogVideoX (In-Domain) and 55.51% on Self-Forcing (Out-of-Domain). ProDet also struggles with Self-Forcing, recording 79.39% AUC.

Table 53. Training from Scratch Average Precision (AP %) Breakdown on SF-DFD. *Frame-level detector.

Detector	In-Domain				Out-of-Domain		
	CogVideoX	SkyReels-V2	Wan2.1	Mean	Self-Forcing	MAGI-1	Mean
RECCE*	91.12	97.59	96.63	95.11	96.08	86.99	91.54
ProDet*	81.46	95.87	91.56	89.63	92.70	76.51	84.61
UCF*	89.46	94.95	93.69	92.70	93.63	84.35	88.99
Effort*	92.29	95.73	95.80	94.61	95.29	78.92	87.11
AltFreezing	97.85	99.33	98.65	98.61	96.78	98.05	97.42
FTCN	94.34	97.72	96.06	96.04	97.22	97.78	97.50
GenConViT	70.96	93.91	91.95	85.61	82.09	51.77	66.93
DFD-FCG	74.72	82.84	83.56	80.37	84.89	70.04	77.47

Table 53 reflects the difficulty in ranking unseen artifacts. GenConViT's AP on Self-Forcing is 82.09%, and on MAGI-1 it falls to 51.77%. Ideally, seen generators like CogVideoX should yield high AP, yet GenConViT records only 70.96%. Also AltFreezing remain stable, with AP $> 96\%$ across all five generators.

Table 54 shows that threshold stability varies by architecture. AltFreezing maintains $> 92\%$ accuracy on both seen (Wan2.1) and unseen (MAGI-1) generators. ProDet shows a specific weakness to Self-Forcing, dropping to 67.46% accuracy compared to 90.64% on SkyReels-V2. GenConViT and DFD-FCG perform near random chance ($\sim 50 - 55\%$) across all generator types in this split.

Table 55 quantifies the separation capability. GenConViT exhibits high error rates on Out-of-Domain generators:

Table 54. Training from Scratch Accuracy (Acc %). Breakdown on SF-DFD. Evaluated at threshold 0.5. *Frame-level detector.

Detector	In-Domain				Out-of-Domain		
	CogVideoX	SkyReels-V2	Wan2.1	Mean	Self-Forcing	MAGI-1	Mean
RECCE*	81.94	84.13	83.81	83.39	79.22	83.29	81.31
ProDet*	74.98	90.64	84.83	85.26	67.46	83.48	76.36
UCF*	77.52	78.73	78.10	78.56	75.35	78.12	76.96
Effort*	62.43	63.33	63.29	65.46	61.48	63.02	63.47
AltFreezing	93.13	94.70	94.01	90.29	92.23	93.95	91.26
FTCN	81.86	90.67	87.05	89.16	89.40	86.53	89.28
GenConViT	52.76	53.03	52.88	55.37	50.74	52.89	53.96
DFD-FCG	47.34	53.10	50.94	54.15	51.60	50.46	52.88

Table 55. Training from Scratch Equal Error Rate (EER %). Breakdown on SF-DFD. Lower values indicate better performance. *Frame-level detector.

Detector	In-Domain				Out-of-Domain		
	CogVideoX	SkyReels-V2	Wan2.1	Mean	Self-Forcing	MAGI-1	Mean
RECCE*	13.93	7.34	8.72	10.13	19.23	10.00	14.68
ProDet*	21.64	9.33	14.32	13.54	26.77	15.10	20.16
UCF*	14.03	7.02	8.63	11.80	20.63	9.89	16.22
Effort*	14.69	10.58	10.65	12.55	28.31	11.97	20.43
AltFreezing	5.63	4.17	5.01	10.85	7.72	4.94	9.29
FTCN	13.77	7.72	11.48	10.22	8.97	10.99	9.60
GenConViT	28.37	12.40	13.77	22.87	47.11	18.18	34.99
DFD-FCG	28.82	26.74	24.31	26.39	36.46	26.62	31.43

47.11% on Self-Forcing and 18.18% on MAGI-1. Even among In-Domain generators, CogVideoX proves challenging for ProDet (21.64% EER) compared to SkyReels-V2 (9.33%).

9.4.3. Analysis on SF-CDF

Table 56. Training from Scratch Video AUC (%). Breakdown by Generator on SF-CDF. *Frame-level detector.

Detector	In-Domain				Out-of-Domain		
	CogVideoX	SkyReels-V2	Wan2.1	Mean	Self-Forcing	MAGI-1	Mean
RECCE*	99.47	99.79	99.75	99.49	98.56	99.67	99.03
ProDet*	97.82	99.68	99.16	99.07	91.92	98.89	95.50
UCF*	98.74	99.36	99.13	98.89	96.42	99.08	97.66
Effort*	99.79	99.92	99.92	99.86	98.05	99.88	98.86
AltFreezing	97.22	98.67	98.04	97.46	98.15	97.98	97.81
FTCN	88.82	94.78	93.56	95.76	96.07	92.39	95.92
GenConViT	98.56	99.67	99.99	99.49	92.99	99.41	96.24
DFD-FCG	82.83	82.43	85.66	85.58	73.86	83.64	79.72

Table 56 shows that In-Domain generators generally maintain high detectability (e.g., GenConViT: 99.99% on Wan2.1). However, the Out-of-Domain generator Self-Forcing causes performance drops for specific models: ProDet falls to 91.92% and GenConViT to 92.99%. FTCN shows lower performance on the In-Domain generator CogVideoX (88.82%) compared to the Out-of-Domain Self-Forcing (96.07%).

Table 57 demonstrates that RECCE and Effort achieve $> 97\%$ AP on Self-Forcing (Out-of-Domain). ProDet shows a drop on Self-Forcing (91.00%) compared to SkyReels-V2 (99.19%). DFD-FCG records lower AP values generally, with a minimum of 70.47% on Self-Forcing.

Table 58 evaluates calibration. Most models maintain $> 88\%$ accuracy on seen generators. For the unseen Self-Forcing, ProDet's accuracy decreases to 74.21%, while

Table 57. Training from Scratch Average Precision (AP %). Breakdown on SF-CDF. *Frame-level detector.

Detector	In-Domain				Out-of-Domain		
	CogVideoX	SkyReels-V2	Wan2.1	Mean	Self-Forcing	MAGI-1	Mean
RECCE*	98.53	99.43	99.51	99.15	97.03	99.16	98.09
ProDet*	96.32	99.19	98.70	98.42	91.00	98.07	94.71
UCF*	96.82	98.36	98.11	97.87	94.01	97.76	95.94
Effort*	99.53	99.81	99.82	99.76	97.43	99.72	98.60
AltFreezing	95.41	97.46	96.93	97.19	97.50	96.60	97.35
FTCN*	86.21	94.19	92.58	95.37	96.08	90.99	95.73
GenConViT	98.62	99.68	99.99	99.48	93.33	99.43	96.41
DFD-FCG	78.79	82.91	84.57	85.90	70.47	82.09	78.19

Table 58. Training from Scratch Accuracy (Acc %). Breakdown on SF-CDF. Evaluated at threshold 0.5. *Frame-level detector.

Detector	In-Domain				Out-of-Domain		
	CogVideoX	SkyReels-V2	Wan2.1	Mean	Self-Forcing	MAGI-1	Mean
RECCE*	93.07	93.66	93.75	93.25	91.55	93.49	92.40
ProDet*	86.37	95.23	93.58	92.22	74.21	91.73	83.22
UCF*	89.10	90.10	89.86	89.64	86.60	89.69	88.12
Effort*	93.10	93.41	93.40	93.46	90.83	93.30	92.15
AltFreezing	88.12	89.43	88.79	87.68	89.03	88.78	88.36
FTCN	79.76	86.34	85.17	87.19	86.80	83.76	87.00
GenConViT	90.06	90.30	90.46	90.45	85.71	90.27	88.08
DFD-FCG	46.73	50.15	48.65	50.43	47.88	48.51	49.16

RECCE maintains 91.55%. GenConViT shows a drop on Self-Forcing (85.71%) compared to Wan2.1 (90.46%). DFD-FCG remains at $\sim 50\%$ accuracy.

Table 59. Training from Scratch Equal Error Rate (EER %). Breakdown on SF-CDF. Lower values indicate better performance. *Frame-level detector.

Detector	In-Domain				Out-of-Domain		
	CogVideoX	SkyReels-V2	Wan2.1	Mean	Self-Forcing	MAGI-1	Mean
RECCE*	5.42	3.55	3.06	4.59	8.25	4.01	6.42
ProDet*	8.89	4.16	5.56	5.94	15.74	6.20	10.84
UCF*	5.90	3.07	3.79	5.23	11.38	4.25	8.31
Effort*	2.88	1.97	2.04	2.39	8.10	2.30	5.25
AltFreezing	6.36	3.93	3.93	6.36	6.36	4.74	6.36
FTCN	20.00	12.12	13.63	10.60	10.60	15.25	10.60
GenConViT	6.74	2.81	0.00	3.37	14.04	3.18	8.71
DFD-FCG	23.26	26.16	22.09	22.67	31.40	23.84	27.04

Table 59 highlights the operational limits. GenConViT achieves 0.00% EER on Wan2.1 (In-Domain) but rises to 14.04% on Self-Forcing (Out-of-Domain). Similarly, ProDet records 15.74% EER on Self-Forcing compared to 4.16% on SkyReels-V2. CogVideoX (In-Domain) results in a 20.00% EER for FTCN, which is higher than its result on the unseen MAGI-1 (15.25%).

9.4.4. Analysis on Legacy Benchmarks

To investigate the generalization to unseen datasets after training on the proposed dataset, the models are evaluated on standard legacy benchmarks: FaceForensics++ (FF++), DeepFake Detection (DFD), and Celeb-DF (CDF). The quantitative results, detailed in Table 60, provide insight into the cross-domain transferability of the learned representations.

Overall, the performance indicates a significant domain gap. Effort and AltFreezing achieve the highest mean AUCs, reaching 61.89% and 60.69% respectively, while the

Table 60. Video AUC (%) on FF++, DFD, CDF. Models trained from scratch and evaluated on traditional benchmarks. *Frame-level detector.

Detector	FF++	DFD	CDF	Mean
RECCE*	58.64	54.36	57.01	56.67
ProDet*	55.93	53.84	49.88	53.22
UCF*	58.38	60.00	55.13	57.84
Effort*	71.29	62.41	51.96	61.89
AltFreezing	68.19	57.09	56.78	60.69
FTCN	58.83	52.84	55.78	55.82
GenConViT	76.45	18.60	61.26	52.10
DFD-FCG	56.37	52.09	43.43	50.63

remaining detectors generally perform near the chance level (approximately 50–58%). Notably, GenConViT exhibits inconsistent behavior, showing moderate detection on FF++ (76.45%) but failing to generalize to DFD.